AFFDL-TR-75-150

(12) FC

AD A023628

# BIRD IMPACT FORCES IN AIRCRAFT WINDSHIELD DESIGN

*IMPROVED WINDSHIELD PROTECTION ADVANCED DEVELOPMENT PROJECT OFFICE*
*VEHICLE EQUIPMENT DIVISION AND*
*UNIVERSITY OF DAYTON RESEARCH INSTITUTE*

MARCH 1976

TECHNICAL REPORT AFFDL-TR-75-150
FINAL REPORT FOR PERIOD JANUARY 1975 – JULY 1975



AIR FORCE FLIGHT DYNAMICS LABORATORY
AIR FORCE WRIGHT AERONAUTICAL LABORATORIES
Air Force Systems Command
Wright-Patterson Air Force Base, Ohio 45433

*NOTICE*

*When Government drawings, specifications, or other data are used for any purpose other than in connection with a definitely related Government procurement operation, the United States Government thereby incurs no responsibility nor any obligation whatsoever; and the fact that the government may have formulated, furnished, or in any way supplied the said drawings, specifications, or other data, is not to be regarded by implication or otherwise as in any manner licensing the holder or any other person or corporation, or conveying any rights or permission to manufacture, use, or sell any patented invention that may in any way be related thereto.*

This report has been reviewed by the Information Office (OI) and is releasable to the National Technical Information Service (NTIS). At NTIS, it will be available to the general public, including foreign nations.

This technical report has been reviewed and is approved for publication.

Richard L. Peterson

RICHARD L. PETERSON
Project Engineer
Air Force Flight Dynamics Laboratory

J. P. Barber

JOHN P. BARBER
Project Engineer
University of Dayton Research Institute

FOR THE COMMANDER

Robert E. Wittman

ROBERT E. WITTMAN
Program Manager
Improved Windshield Protection ADPO
Air Force Flight Dynamics Laboratory

| ACCESSION for | | |
|---|---|---|
| NTIS | White Section | ☑ |
| DDC | Buff Section | ☐ |
| UNANNOUNCED | | ☐ |
| JUSTIFICATION | | |
| BY | | |
| DISTRIBUTION/AVAILABILITY CODES | | |
| Dist. | AVAIL. and/or SPECIAL | |
| A | | |

***Copies of this report should not be returned unless return is required by security considerations, contractual obligations, or notice on a specific document.***

AIR FORCE - 19 APRIL 1976 - 200

UNCLASSIFIED

SECURITY CLASSIFICATION OF THIS PAGE (When Data Entered)

## REPORT DOCUMENTATION PAGE

READ INSTRUCTIONS BEFORE COMPLETING FORM

1. REPORT NUMBER: AFFDL-TR-75-150
2. GOVT ACCESSION NO.:
3. RECIPIENT'S CATALOG NUMBER:

4. TITLE (and Subtitle): BIRD IMPACT FORCES IN AIRCRAFT WINDSHIELD DESIGN

5. TYPE OF REPORT & PERIOD COVERED: Final Report, Jan [redacted]-Jun [redacted]975

6. PERFORMING ORG. REPORT NUMBER:

7. AUTHOR(s): Richard L. Peterson, Air Force Flight Dynamics Laboratory
John P. Barber, Univ. of Dayton Research Institute

8. CONTRACT OR GRANT NUMBER(s): F33615-73-C-5027

9. PERFORMING ORGANIZATION NAME AND ADDRESS:
University of Dayton Research Institute
300 College Park Avenue
Dayton, Ohio 45469

10. PROGRAM ELEMENT, PROJECT, TASK AREA & WORK UNIT NUMBERS:
Project No. 2202
Task No. 220203
Work Unit No. 22020303
AF-2202, AF-1456

11. CONTROLLING OFFICE NAME AND ADDRESS:
Air Force Flight Dynamics Laboratory (FEW)
Wright-Patterson Air Force Base, Ohio

12. REPORT DATE: Mar [redacted]976

13. NUMBER OF PAGES: 55 (12) 65 p.

14. MONITORING AGENCY NAME & ADDRESS (if different from Controlling Office):
12) 220303, 14) 75

15. SECURITY CLASS. (of this report): Unclassified

15a. DECLASSIFICATION/DOWNGRADING SCHEDULE:

16. DISTRIBUTION STATEMENT (of this Report)
Approved for public release; distribution unlimited.

17. DISTRIBUTION STATEMENT (of the abstract entered in Block 20, if different from Report)

18. SUPPLEMENTARY NOTES

19. KEY WORDS (Continue on reverse side if necessary and identify by block number)

| | |
|---|---|
| Bird Impact Tests | Steady State Pressure |
| Pressure Transducers | Aircraft Windshields |
| Bird Gun Impact Facility | Aircraft transparent enclosure |
| Hopkinson Bar Force Tests | |

20. ABSTRACT (Continue on reverse side if necessary and identify by block number)

In order to design transparent aircraft windshield and canopy panels which can withstand the impact of birds, and at the same time meet other equally important operational requirements, it is necessary to define the forces generated during the birdstrike event. It is important to define the total force in order to understand the far field structural response; and the local pressure and pressure distribution in order to understand local structural response. The total force as a function of time was measured by impacting birds onto a large

Continued on DD FORM 1473E

DD FORM 1 JAN 73 1473 EDITION OF 1 NOV 65 IS OBSOLETE

UNCLASSIFIED

SECURITY CLASSIFICATION OF THIS PAGE (When Data Entered)

105 400

Abstract contd (from p 1473A)

diameter Hopkinson bar. The local pressures and pressure distribution during the bird impact were measured by flush mounting piezo-electric pressure transducers in a heavy rigid flat plate and impacting the plate/transducer assembly. The forces and pressures are a function of the relative impact velocity and angle, the weight and average density of the bird and the stiffness of the impacted structure. In order to define the temporal and spatial distribution of the bird impact forces, the Air Force Flight Dynamics Laboratory has initiated a substantial parametric bird/plate impact test program. These tests are being conducted at Air Force Materials Laboratory/ University of Dayton Research Institute and the Arnold Engineering Development Center and cover a velocity range from 30 m/s to 350 m/s, impact angles from 15° to 90° in trajectory and bird weights from 0.05 kg to 3.6 kg. The results at the 90° test angle indicate that: (1) birds behave essentially as a fluid during impact; (2) birds do not bounce at impact - the impulse is equal to the initial impact momentum; (3) the high frequency component of pressure superimposed on the base pressure-time pulse is caused by breakup of the bird flesh and inhomogeneities in the bird; and (4) the duration of loading is approximately equal to the 'squash up' time.

1473B

# FOREWORD

This report summarizes the results of the second phase of the Air Force Flight Dynamics Laboratory (AFFDL) Improved Windshield Protection ADPO bird impact loading program. The bird impact test programs were conducted by the University of Dayton Research Institute at the Air Force Materials Laboratory (AFML), Wright-Patterson Air Force Base, Dayton, Ohio, under Contract F33615-73-C-5027; and by the Arnold Engineering Development Center (AEDC), Arnold Air Force Station, Tennessee, under Project Order 1456-75-00725.

The work was accomplished under Project 2202, "Improved Windshield Protection Development Program;" Task 220203, "Improved Windshield Design Criteria;" and Work Unit 22020303, "Transparent Enclosure Design Criteria." The bird impact testing programs were accomplished from January 1975 to July 1975. Mr. Richard L. Peterson (FEW) was the technical monitor for the bird impact test support programs for the Air Force Flight Dynamics Laboratory.

Dr. John P. Barber of the University of Dayton Research Institute was responsible for operation of the AFML small bird gun impact test facility including reduction and analysis of the bird impact data. Mr. James Y. Parker of the Arnold Research Organization was responsible for operation of the AEDC large bird gun impact test facility including reduction and correlation of the bird impact data.

The authors are indebted to the following Air Force and industry personnel who contributed to this effort. Major Dale N. Holasek of the Arnold Engineering Development Center; George W. Robertson Jr. and Howard G. Harris of the Arnold Research Organization; Dr. Alan K. Hopkins, Lt. James S. Wilbeck of the Air Force Materials Laboratory, Henry R. Taylor, James Green and David Osborn of the University of Dayton Research Institute.

This report was submitted by the authors on 1 December 1975.

TABLE OF CONTENTS

# LIST OF ILLUSTRATIONS

LIST OF ILLUSTRATIONS - CONTINUED

LIST OF ILLUSTRATIONS - CONCLUDED

# SECTION I

# INTRODUCTION

Bird impacts on aircraft windshields and canopies may produce damage or catastrophic failure which can result in mission abortion, loss of the aircraft and/or loss of crewmembers. Aircraft birdstrikes have greatly increased over the last 20 years principally because of increased speeds in jet engine aircraft and the advent of low altitude high speed penetration missions. The engines, windshields, and canopies have proven to be the most vulnerable portions of an aircraft.

Since 1966 the U.S. Air Force has lost at least eleven aircraft worth over 61 million dollars due to bird impacts on transparent enclosures. These include the loss of a T-37B with one fatality, three T-38s with two fatalities, two F-100s with one fatality, and five F-111s with, fortunately, no fatalities. In addition to the $61 million loss in airframes, and the incalculable loss due to fatalities, an estimated $20 million has been spent in repair costs during the period 1966 through 1972. Further, the role of bird impacts in aircraft losses in Southeast Asia is not fully known.

In order to utilize analytical windshield design techniques and computer programs in the windshield design process, it is necessary to first adequately understand how a windshield is loaded by a bird during the birdstrike event. This involves determining the local pressure and

pressure distribution (both temporal and spatial) in order to understand local structural response, and the total force in order to understand the far field structural response.

The Air Force Flight Dynamics Laboratory (AFFDL) is currently conducting several R&D programs at Arnold Engineering Development Center (AEDC) and the Air Force Materials Laboratory/University of Dayton Research Institute (AFML/UDRI) which will define local pressure and total force on a flat rigid plate for various bird weights and velocities, and for various angles of impact.

# SECTION II

# EXPERIMENTAL TECHNIQUES

Bird/plate impact experiments are conducted using whole, recently deceased birds (chickens) ranging in size from 0.05 kg to 3.6 kg. The AEDC facility is used for bird weights above 0.25 kg. The birds must be launched intact at velocities from 30 m/s to 350 m/s. Some of the pertinent launcher design considerations and constraints are:

a. Birds must be prevented from breaking up during launch by use of appropriate saboting and/or bagging techniques.

b. Acceleration must be kept sufficiently low to prevent destruction of the bird.

c. The bird must separate freely from the sabot.

d. The sabot must be stopped in the launch tube or diverted from the bird trajectory to prevent the sabot from impacting the target.

e. Acceleration must be removed from the bird for a sufficient period of time to permit the bird to 'relax' before impact.

## 1. AFML/UDRI FACILITY DESCRIPTION

a. The Range - The AFML/UDRI range (Reference 1) consists of an 8.90 cm bore x 4.27 m long powder driven gun, a blast tank and a target

tank as shown in Figure 1. Each end of the gun tube is threaded to accept a breech block at the breech end and a sabot stopper at the muzzle end. Four longitudinal slits, 46 cm long, were machined, near the muzzle, in the gun tube to vent the powder gas and permit the sabot to begin deceleration before striking the sabot stopper. The propellant powder used was a small bore powder identified as "Bullseye."

The breech block incorporates a soft launch buffer technique which generates a low but constant acceleration pressure behind the projectile until the pressure is relieved by the longitudinal slits at the muzzle. The buffer system consists of a chamber in the breech block into which the powder gas expands. The output port of the chamber is necked down to restrict gas flow into the gun.

During a test, the range is evacuated to an air pressure of 5 torr to assure repeatable bird orientation at impact. The sabot is fabricated from high density polyethylene. A 1.27 cm thick hard rubber ring attached to the sabot stopper plate acts as a pad for the sabot wall to strike. A conical steel spreader ring with an interior diameter of 0.65 cm greater than the diameter of the sabot pocket is attached to the stopper plate as shown in Figure 2. The spreader ring cuts into the wall of the sabot forcing most of the wall to spread outward and into the stopper plate. Only the outer portion of the sabot wall is deformed and the pocket remains intact. The pocket in the sabot is sized to accommodate birds weighing 0.05 kg to 0.15 kg. Satisfactory sabot separation is achieved and there are no secondary impacts of sabot material

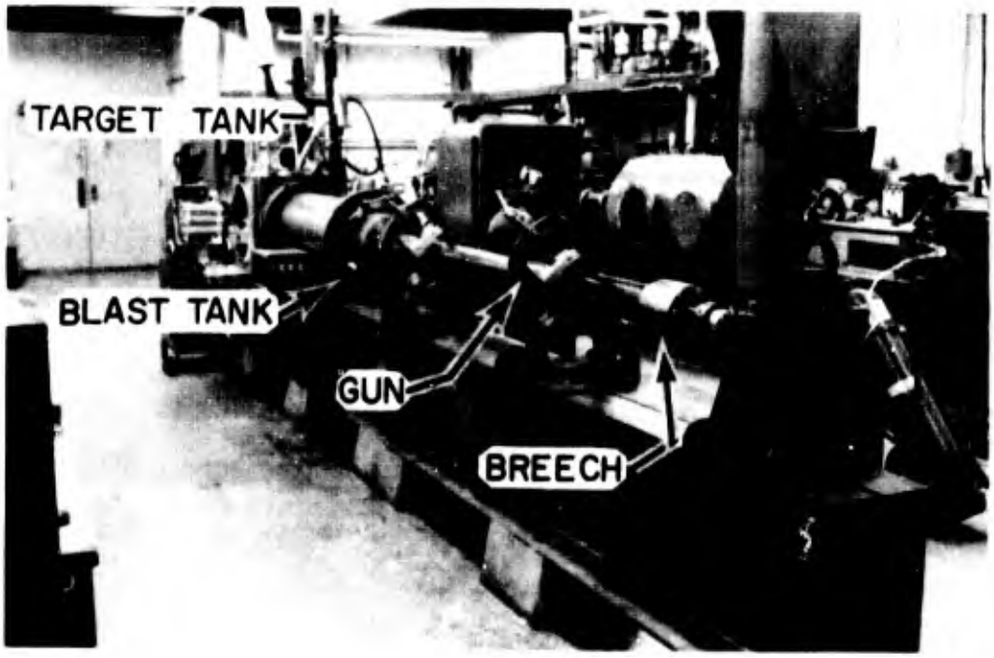


Figure 1. Overall View of AFML/UDRI Bird Range Facility

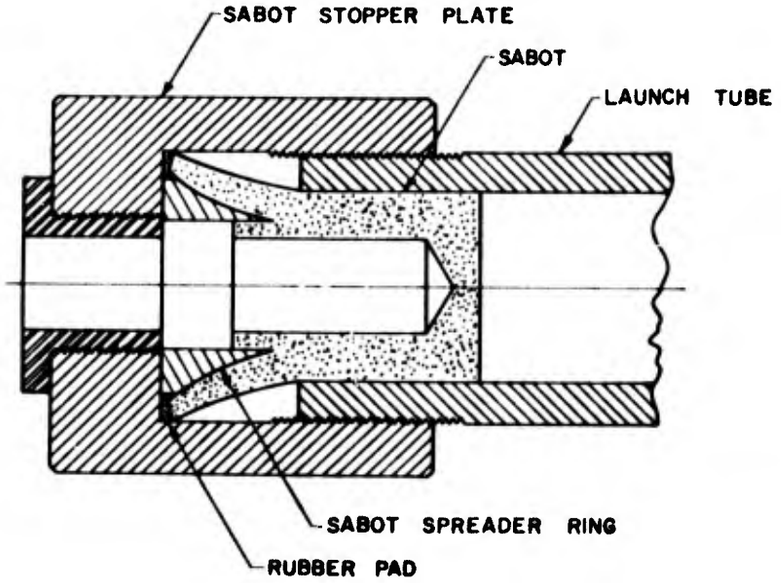


Figure 2. Sabot Stopper

on the target surface. The bird releases without any apparent damage or disruption to its attitude or flight path as evidenced by the x-radiographs and photographs.

b. Velocity Measurement System - Velocity is calculated from the time of flight as the bird passes through two pairs of laser light beams. The time interval is measured with a digital time interval counter. Two laser beams are aligned at each station to form a triangular plane perpendicular to the projectile trajectory with the beams converging at the element of a photomultiplier tube. Because the beams are independent, they must both be interrupted simultaneously to produce a signal of sufficient amplitude to overcome the bias on a built-in pulse amplifier and generate a signal. The use of two lasers at each velocity station is necessary to assure that the velocity of the main body of the bird is measured and not the velocity of loose feathers or debris. Photographs and x-radiographs verify the reliability of this trigger system. The accuracy of the velocity measurement system is ±1%.

c. Photograph and x-radiography - Each bird launched is x-rayed and photographed immediately prior to impact to verify that it was properly oriented and intact. In addition, high speed cinematography of the bird during impact is obtained on selected shots to aid in the description and understanding of the bird breakup. The x-ray and light sources are triggered from the output of the first interrupted laser beam velocity measuring station. All birds are launched tail leading and impact the plate in that orientation. From the x-radiographs, no breaking or crushing of bones during launch for muzzle velocities of up to 350 m/s is observed.

A xenon flash tube light source and 10 cm x 12.5 cm camera are used to obtain photographs of the bird prior to impact to verify the x-radiographic results. Typical photographs are shown in Figure 3.

A full framing 16 mm Fastax camera at a framing rate of 7500 frames per second is used to record the impact process in order to observe bird breakup and debris distribution during and after impact.

d. Hopkinson Bar Study - Hopkinson bars have been used over the last 50 years for measuring force-time histories of impulsive events. The basic concept on which a Hopkinson bar operates is that a force rapidly applied to the end of a homogeneous bar of elastic material will generate a stress wave that propagates along the bar at constant (near sonic) velocity. The stress wave can be detected at any point along the bar by placing a strain gage on the bar surface and monitoring the output. The strain-time history is related to the instantaneous force, F, applied to the end of the bar through the Youngs modulus, E, of the bar material and the cross-sectional area of the bar, A, as $F = \varepsilon EA$, where $\varepsilon$ is the measured strain as a function of time.

This principle is applied to determine the force-time history of a bird striking a rigid plate as follows. The birds are launched against the end of a long aluminum bar on which strain gages are mounted 10 diameters down the bar from the impacted end. The resulting strain pulse in the bar is recorded and related to the stress pulse. The bar must be long enough to assure that the entire stress pulse from the impact is recorded before a reflected wave from the far end of the bar

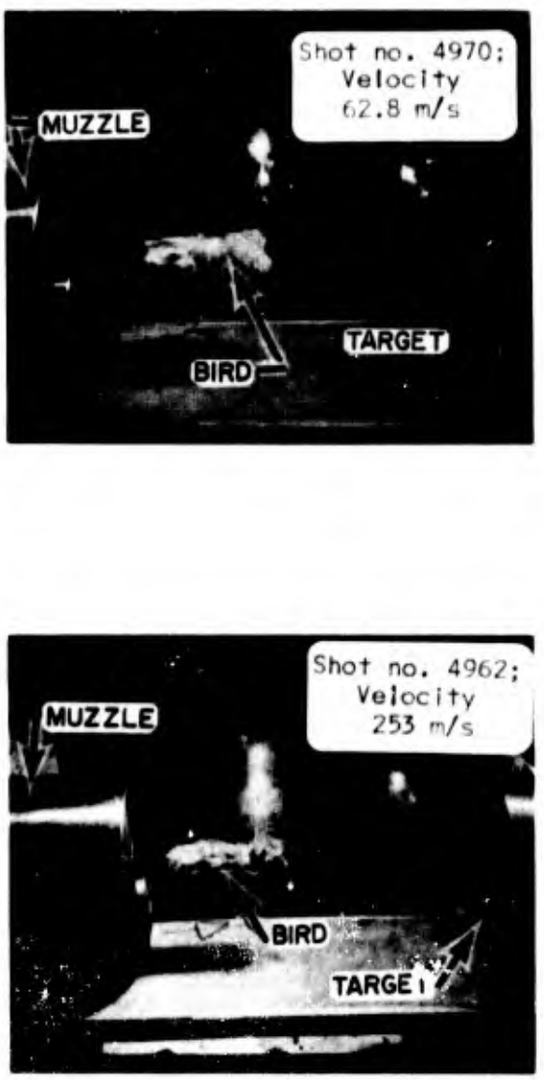


**Figure 3. Photographs of Launched Birds**

can propagate back to the strain gage. A 3.66 m long, 7.62 cm diameter rod of 7075 T6 aluminum was chosen. The 7.62 cm diameter is the minimum which would permit the lateral expansion of the bird upon impact without allowing material to flow around the rod and continue down-range. Two strain gages are mounted on opposite sides of the bar 76.2 cm (10 rod diameters) from the impact end as shown in Figure 4. The two gages are connected in series to a strain gage bridge such that the signal from each gage is added to double the sensitivity of the system. Rod bending, which occurs if the impact is slightly off center, produces compression in one gage and tension in the other; the signals then subtract and the bending signal is rejected.

Considerable thought was given to techniques for mounting the bar in the ballistic range. Rigid longitudinal restraint of the bar introduces error signals into the data while insufficient restraint of the bar permits the bar to recoil and move down the range. The solution chosen is to connect the front end of the bar to the ballistic range with a rubber boot which allows almost total freedom of motion while permitting the range to be evacuated. The bar is loosely supported along its length on teflon rings which provide good lateral support and virtually no longitudinal constraint. The rear end of the bar is butted against a rigid constraint to prevent gross motion. A photograph of the Hopkinson bar mounted on the range is shown in Figure 5.

Strain data is recorded by observing the output of a standard strain gage bridge with an oscilloscope and photographing the resultant trace. A cine camera is also used to view the impact of birds striking

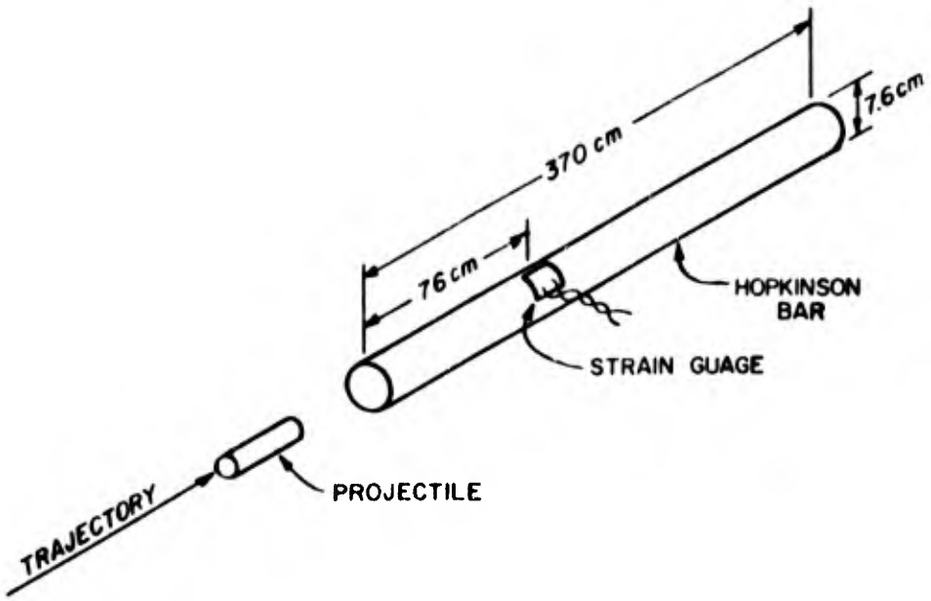


Figure 4. A Hopkinson Bar as Configured to Measure Impact Forces


Figure 5. The Hopkinson Bar Mounted on the AFML/UDRI Range

the end of the rod. The films show clearly that the birds are totally stopped by the rod; no material flows around the rod and continues in its original direction. In addition, it is observed that 'bounce' is negligible and the bird material flows radially away from the impact point along the end surface of the rod.

e. Pressure Measurement - Piezo-electric quartz pressure transducers which employ a compact impedance converter physically located in the coaxial line close to the crystal are used to sense local pressure in these experiments. Since these transducers are not designed for impact testing, considerable experimentation and calibration was necessary to verify their operation. A calibration method for the transducers was developed to verify the applicability of the manufacturer's calibration data to the unidirectional axial loads anticipated. A device was fabricated to enable unidirectional axial loads, similar to the bird/plate impact loads, to be applied to the transducer and measurements were taken to determine the response of the transducers. It was concluded that the transducers provided reliable, accurate pressure data over the range of pressures and frequencies expected.

The target, a 15.25 cm diameter 5.10 cm thick steel disk, is mounted on the tank wall approximately 36 cm from the gun muzzle as shown in Figure 6. The transducers are flush mounted at 1.27 cm radial intervals in the steel target disk. The disk is supported by a 10.16 cm diameter, 1.27 cm wall tube, which is welded to a 3.81 cm thick flange. This design provides a rigid target support while permitting ease of access to the transducers.


Figure 6. The AFML/UDRI Pressure Plate Showing the Pressure Transducers Flush Mounted on the Impact Surface

A series of bird (chicks) impact experiments against the instrumented target were conducted over a velocity range of 30 m/s to 300 m/s. Bird weights range from 0.05 kg to 0.15 kg. The target was positioned at 25°, 45°, and 90° to the bird trajectory during the test program. The pressure-time pulse was recorded using oscilloscopes. The pressure pulse was filtered to 10 kHz to eliminate the majority of the high frequency signal. The results are reported in Section III.

## 2. AEDC FACILITY DESCRIPTION

a. The Range - The AEDC bird launcher (Reference 2) is an air operated gun consisting of a driver, launch tube, breech section, and sabot stripper tube as shown in Figures 7 and 8. The launcher consists of a 9.45 m long driver having a 20.3 cm diameter bore with a volume of 0.329 $m^3$. The bird and its sabot are loaded between the driver and the launch tube immediately forward of a double diaphragm section. The bird is launched by charging the driver with air to the desired pressure while simultaneously charging the volume between the two diaphragms to some intermediate pressure. The volume between the diaphragms is then vented whereupon the diaphragms are overpressured and rupture, propelling the sabot containing the bird down the launch tube. The diaphragms are made of Mylar and vary in thickness from 0.13 cm to 0.36 cm depending upon the desired burst pressure.

The test area consists of a 6.9 m by 9.7 m covered concrete pad (reference Figure 8) upon which are set steel H-beams used for mounting targets. The area is equipped with a high pressure water hose with which bird debris is washed into a container located underneath the

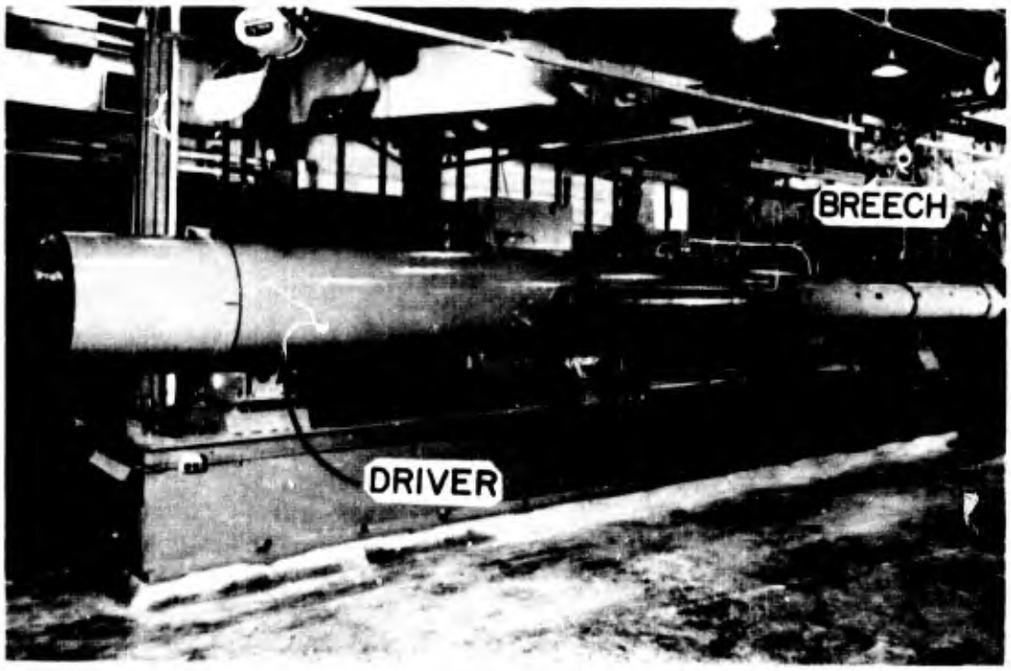


Figure 7. AEDC Bird Impact Launcher

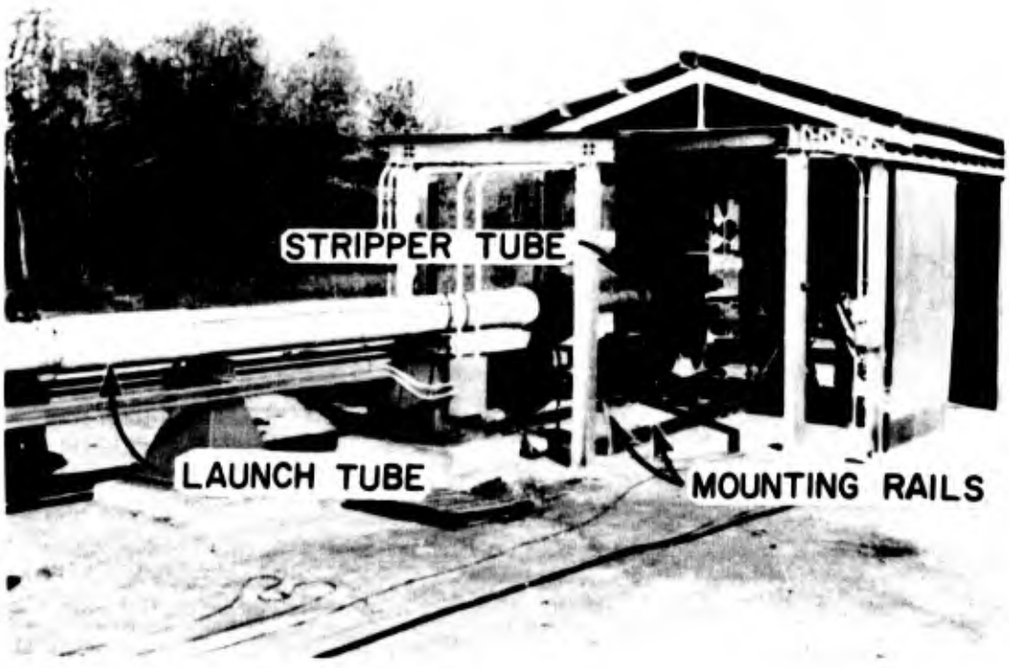


Figure 8. AEDC Bird Impact Facility Test Area

floor near the back edge of the pad. The target is located 7.6 m from the stripper muzzle. The accuracy of the launcher in striking the designated target point with the projectile is ±2.5 cm. The birds used are chickens, and they are packaged in a nylon bag before insertion into the sabot in order to prevent aerodynamic breakup during flight to the target. Balsa wood sabots are used because of their light weight, low cost, relatively high strength, ease of manufacture, and simplicity of removal from the stripper after the shot. The density of the balsa wood varies and the denser high strength material is used for higher speed shots.

The sabot is prevented from striking the target by a tapered stripper tube attached to the muzzle of the launch tube. The stripper tube as shown in Figure 9 consists of a 0.61 m long vent section to allow escape of the driving gas, followed by a 3.05 m length of pipe with a taper machined in the bore. The taper reduces from the 17.8 cm launch tube bore diameter down to approximately 13.3 cm diameter at the muzzle. The sabot is removed from the stripper after the shot by driving it back into the vent section, then splitting it into pieces small enough to be removed between the vent section guide rails.

b. Test Instrumentation - Test instrumentation includes a projectile velocity measuring system, piezo-electric pressure transducer/recording system, and general still and cine picture coverage of the impact event.

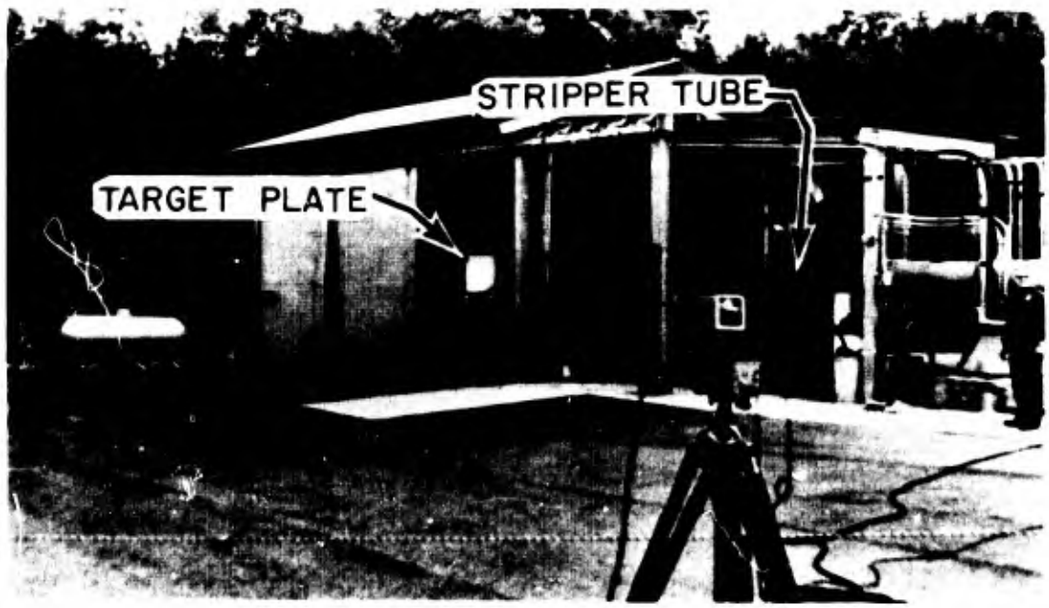


Figure 9. AEDC Target Plate at 90°

The primary system for measuring projectile velocity consists of two x-ray stations located a known distance apart along the flight path between the launcher muzzle and the target. Each x-ray pulser is triggered by breaking a 24 gauge copper wire in an electrical break-wire system. The time between firing of the pulsers is recorded with a digital chronograph and, using this time together with the distance measured between images of the projectile on the x-ray film (after corrections for point source parallax), velocity is determined. The velocity measuring system is mounted on an instrumentation dolly with the first station located approximately 1.07 m from the muzzle of the stripper tube. The distance between the two x-ray stations is 2.13 m. The accuracy of this velocity measuring technique is better than ±1%.

c. Pressure Measurement - Piezo-electric quartz pressure transducers which employ a compact impedance converter in the coaxial line close to the crystal are used to sense impact pressure. FM magnetic tape recorders are used to record the pressure data.

The target, a 76 cm x 76 cm steel plate, 10 cm thick, is mounted on the birdstrike fixture approximately 7.62 m from the gun muzzle (reference Figure 9). The target plate can accommodate up to 29 pressure transducers positioned as shown in Figure 10.

d. Test Program - A series of full size bird (chicken) impact experiments against the instrumented target are scheduled over a velocity range of 90 m/s to 350 m/s. Bird weights range from 0.9 kg to

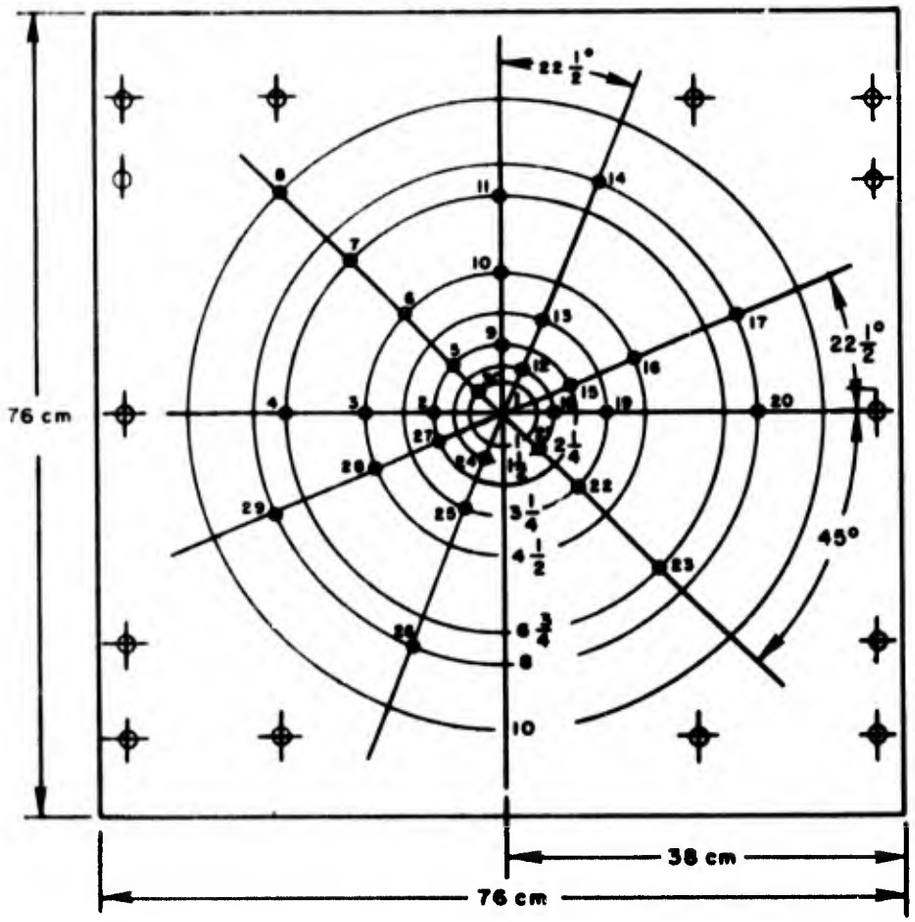


Figure 10. Location of Pressure Transducers in AEDC Target Plate

3.6 kg. The target is positioned at 15°, 30°, 45°, 60°, 75°, and 90° to the impact trajectory during the test program. The pressure-time pulses are recorded on FM magnetic tape for data reduction at a later date. Oscillograph traces from the FM system are obtained for quick check reference. Selected high speed cine and still coverage are also accomplished.

# SECTION III

# EXPERIMENTAL RESULTS

This section reports and discusses the results obtained to date. The AFML/UDRI and AEDC results are reported separately and a comparison is made at the end of this section.

## 1. AFML/UDRI RESULTS

a. Hopkinson Bar Results - A series of bird impact tests on the Hopkinson bar were conducted. The bird masses were in the range from 0.05 kg to 0.15 kg. Impact velocities ranged from about 30 m/s to almost 300 m/s.

The force-time record for a typical bird impact is shown in Figure 11. The force rises rapidly to a maximum and then falls linearly for some time followed by an exponential drop to zero. The total duration of the impact is closely approximated by the time required for the bird to travel its own length at the impact velocity.

The area under the force-time curve is simply the impulse imparted to the target during the impact. If the bird does not bounce, the impulse should be exactly equal to the initial bird momentum. The force-time records from the Hopkinson bar were integrated to yield impulse and the measured impulse as a function of impact momentum is displayed in Figure 12. There is no evidence of bird bounce and resultant systematic

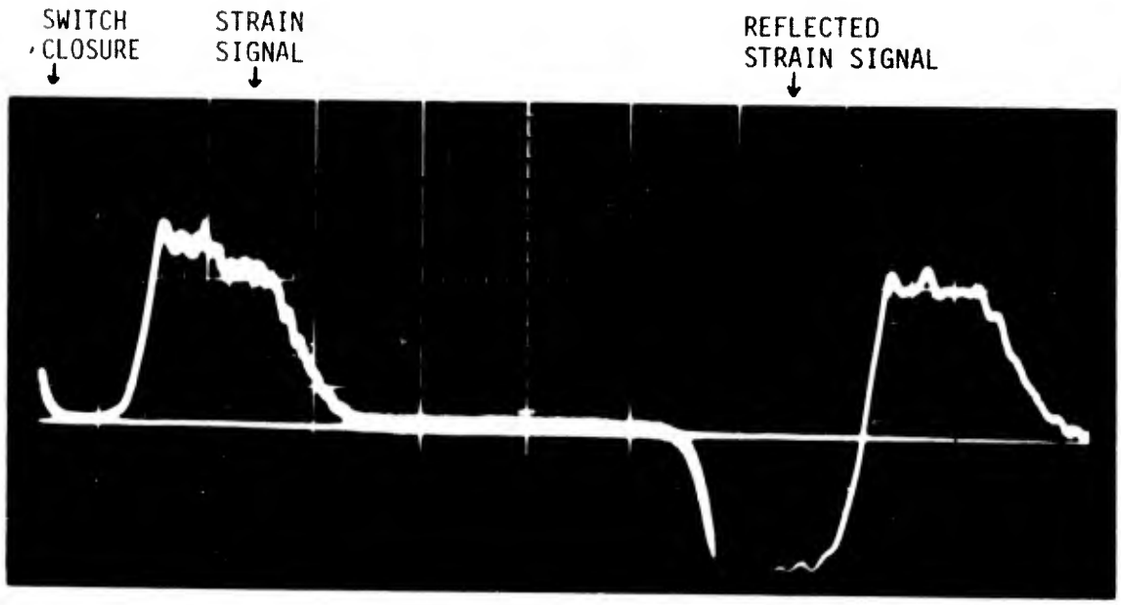


Figure 11. An Oscillograph of the Strain Gage Output on a Hopkinson Bar During a Bird Impact

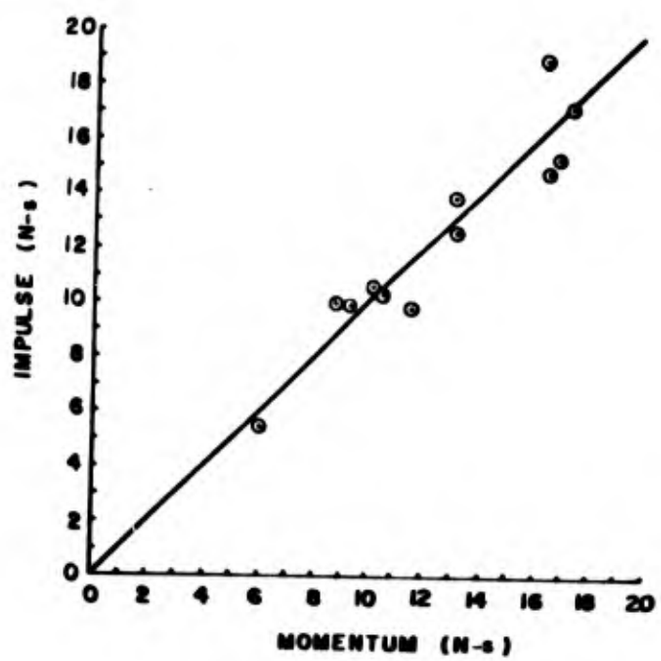


Figure 12. Impulse Vs Impact Momentum for Birds Impacted on a Hopkinson Bar

impulse augmentation. The entire momentum of the bird is converted to impulse.

If the bird does not decelerate during impact (i.e., the impact is supersonic) then the duration of the force-time pulse should be equal to the time it takes for the bird to 'squash up'. The 'squash up' time is given by the length of the bird divided by the impact velocity. The measured results are shown in Figure 13. Within the experimental accuracy the results indicate that the duration is equal to or slightly greater than the 'squash up' time. The bird therefore decelerates very little, if any during the impact.

The impulse imparted to the target is given by the initial momentum, $P = mv$, of the bird where m is the bird mass and v is the impact velocity. The time, t, over which this impulse is imparted is the 'squash up' time, $t = \ell/v$, where $\ell$ is the length of the bird. The average force, $F_{avg}$, is therefore given by

$$F_{avg} = P/t = mv^2/\ell. \tag{1}$$

The peak force is higher than the average force by some factor. If the basic 'shape' of the force-time pulse remains constant, independent of bird mass and velocity, then that factor should remain constant. This may be formalized by introducing a nondimensional force

$$\bar{F} = F/F_{avg}. \tag{2}$$

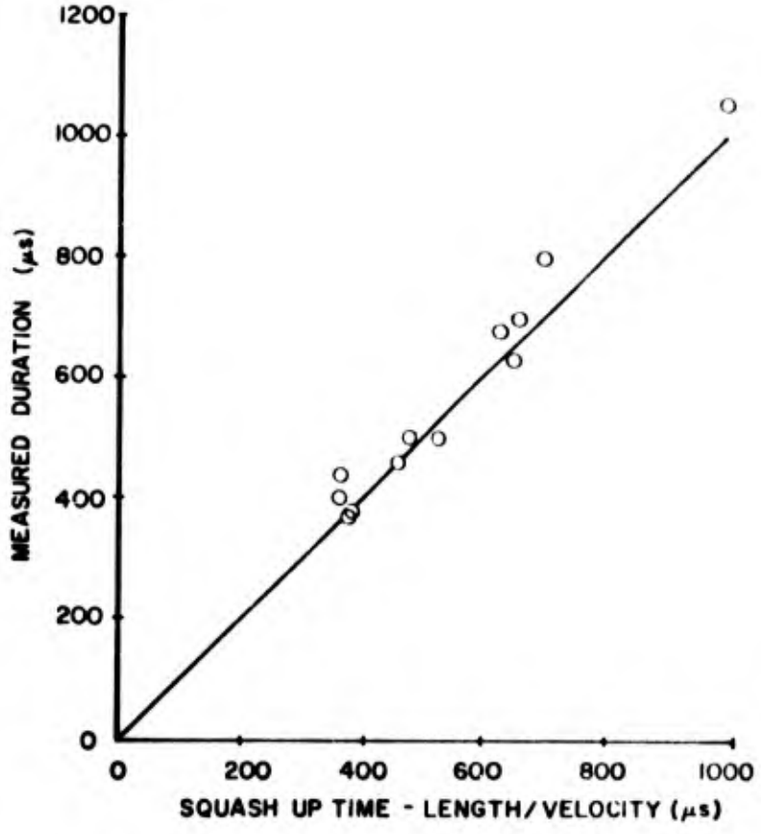


Figure 13. Force Time Pulse Duration Vs Calculated "Squash Up" Time for Bird Impacts on a Hopkinson Bar

The peak force was measured in the Hopkinson bar records and the results in terms of the nondimensional peak force, $\bar{F}_{peak}$, are shown in Figure 14. From Figure 14 it is apparent that although there is considerable scatter, particularly at low velocity, the nondimensional peak force would be exactly 2 if the force-time curve was 'triangular.' A large number of curves have been examined, and they are roughly 'triangular.' The force rises linearly to a peak force of twice the average and falls linearly to zero.

b. Pressure Plate Results - More than 100 impact tests were conducted on the pressure plate at AFML/UDRI to determine the manner in which a bird loads a plate during impact. The output from the pressure transducers were recorded with oscilloscopes. Typical pressure-time records at the center-of-impact are shown in Figure 15. Pressures of 100 $MN/m^2$ and pressure durations of the order of hundreds of microseconds are typical. The recorded pressure time pulse can be described as a relatively low frequency 'base' pressure pulse on which is superimposed a high frequency pressure variation as illustrated in Figure 16. The base pressure profile remains similar from shot to shot, although amplitude and duration vary with velocity and bird size. The high frequency component varies in frequency and amplitude from shot to shot and appears to have little repeatable structure. Acceleration measurements on the impact plate verified the ability of the acceleration compensation mechanism in the pressure transducers to adequately reject high amplitude, high frequency shock accelerations. A number of impact tests conducted using 'RTV' (GE RTV-560) rubber cylinders generated accelerations similar to those produced by birds, but the 'RTV' pressure

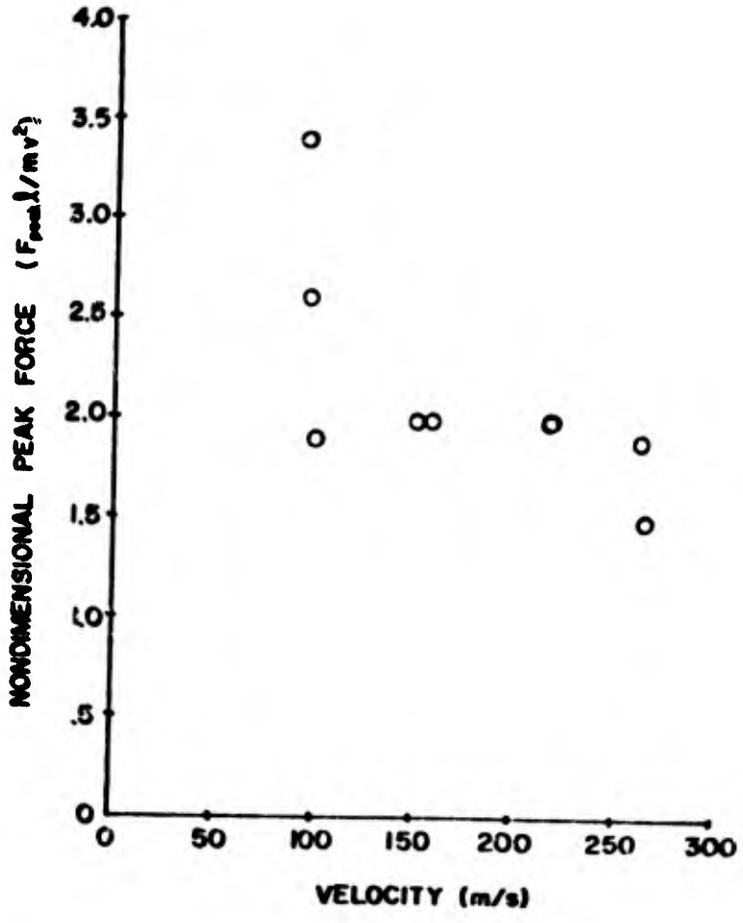


Figure 14. Nondimensional Peak Force Vs Velocity for Bird Impacts on a Hopkinson Bar

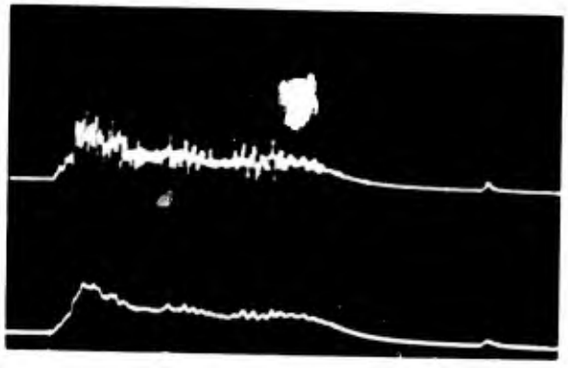

Shot no. 5404; velocity 109 m/s;
horizontal scale 200 μs/cm; vertical scale 12.3 $MN/m^2/cm$;
upper trace unfiltered; lower trace filtered

Shot no. 5399; velocity 199 m/s;
horizontal scale 100 μs/cm; vertical scale 24.5 $MN/m^2/cm$;
upper trace unfiltered; lower trace filtered

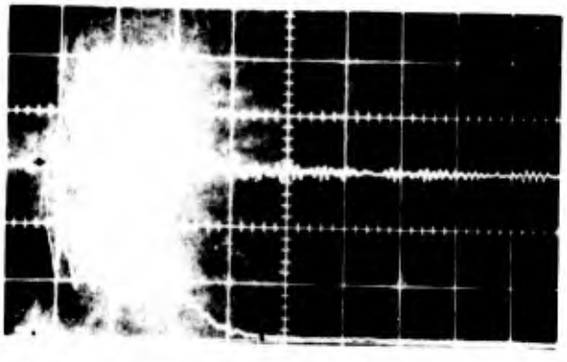

Shot no. 5396; velocity 279 m/s;
horizontal scale 100 μs/cm; vertical scale 49.0 $MN/m^2/cm$;
upper trace unfiltered; lower trace filtered

Figure 15. Centerline Pressure Transducer Outputs for AFML/UDRI Target Disk

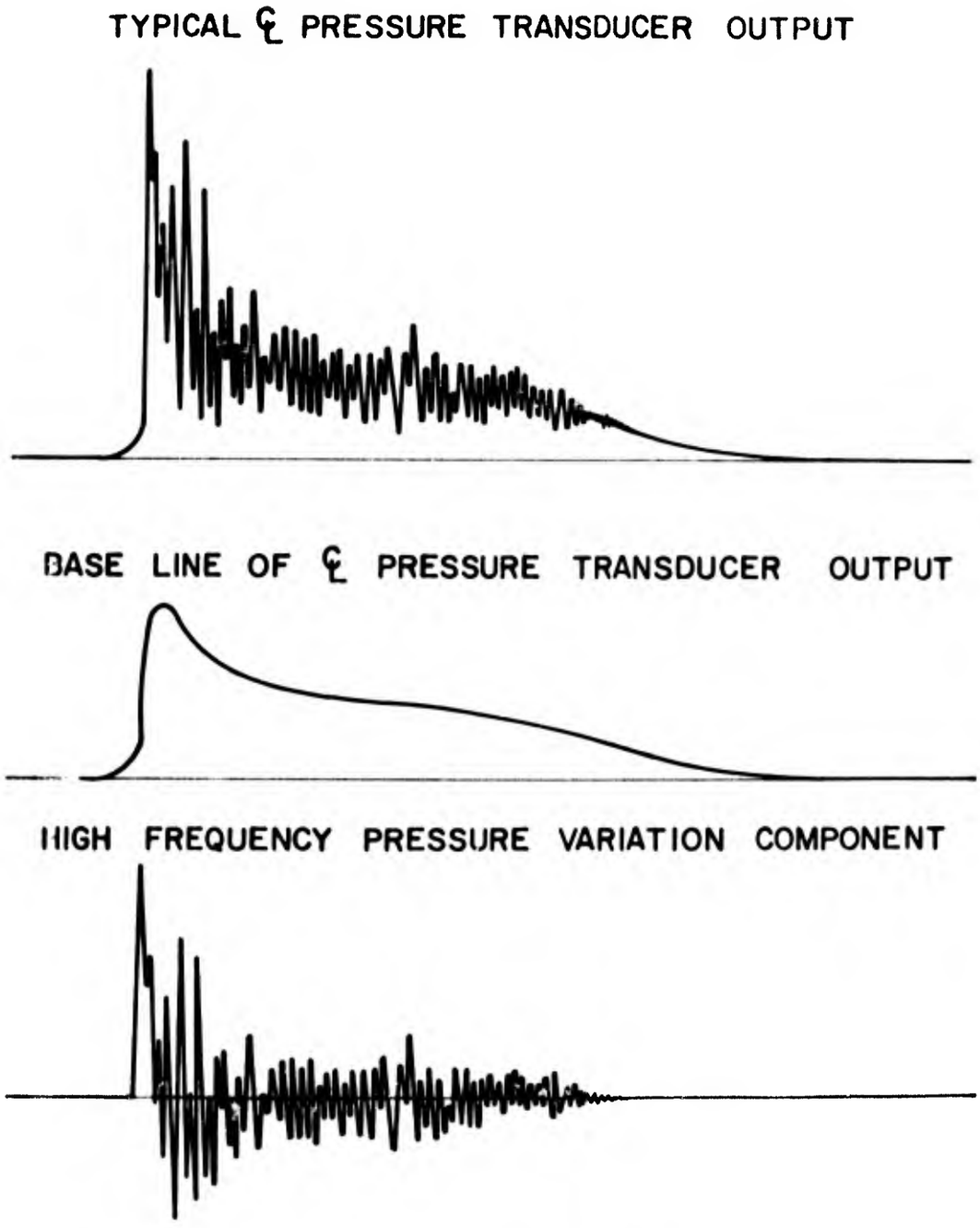


Figure 16. Typical Components of Impact Pressure for Bird Impacts

data lacked the high frequency content as indicated in Figure 17. The high frequency pressure component of real bird impacts must therefore be regarded as a particular and real characteristic of bird impact and not just instrumentation noise. Further tests were conducted with boneless beef and the results are shown in Figure 17. The similarity in the high frequency content of beef and birds indicates that the high frequencies are related to the fracturing of flesh. Other tests on RTV-560 with large inhomogeneities introduced (voids, plastic rods, etc) indicate that inhomogeneities contribute a small portion of the noise.

If the bird is regarded as a homogeneous fluid-like material characterized by some density and the physical dimensions of the bird, then the flow of the bird material on the rigid plate generates the pressure observed. When the bird initially impacts the plate, a plane stress wave propagates into the bird. The pressure at the center-of-impact rises rapidly to the uniaxial impact stress (the Hugoniot). The edge of the bird is a free surface and a release wave propagates radially in towards the center causing the pressure to decay. 'Steady' radial flow is established and the center-of-impact pressure remains steady at $1/2\ \rho v^2$. The end of the bird reaches the plate and the pressure then falls to zero. There is a marked similarity between the filtered bird pressure trace and the RTV (homogeneous) pressure trace shown in Figure 17. The 'steady state' pressure generated is close to that which might be expected from a fluid of specific gravity somewhat less than one. Local density variations and/or large local material differences (for example bones) in the bird in addition to flesh breakup contribute to the high

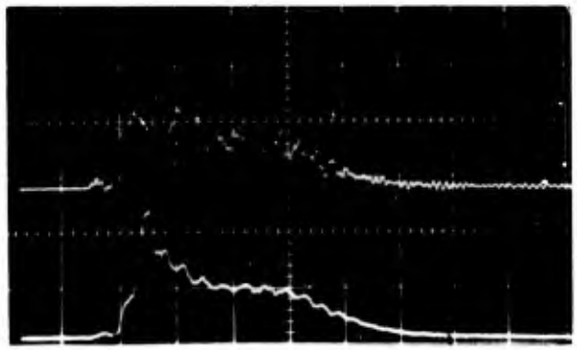

Bird impact; shot no. 5399; velocity 199 m/s;
horizontal scale 100 μs/cm; vertical scale 24.5 $MN/m^2$/cm;
upper trace unfiltered; lower trace filtered

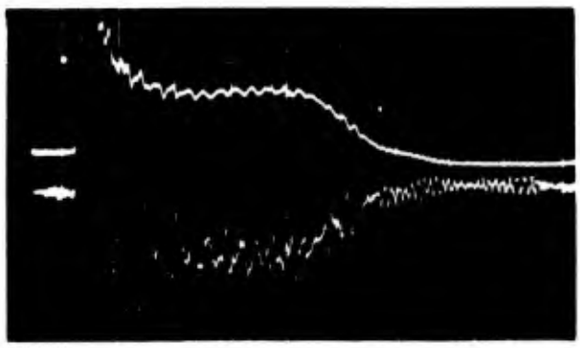

Beef impact; shot no. 5306; velocity 174 m/s;
horizontal scale 100 μs/cm; vertical scale 11.9 $MN/m^2$/cm;
upper trace filtered; lower trace unfiltered

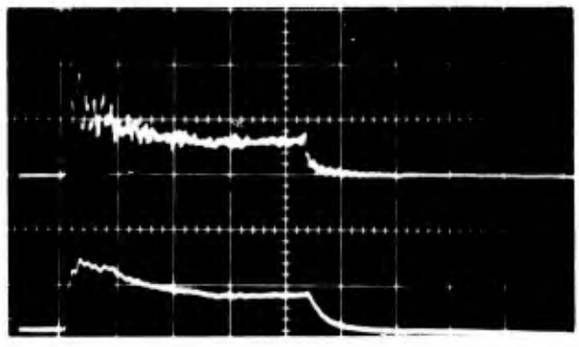

RTV-560 impact; shot no. 5369; velocity 192 m/s;
horizontal scale 100 μs/cm; vertical scale 23.9 $MN/m^2$/cm;
upper trace unfiltered; lower trace filtered

**Figure 17. Pressure Transducer Output for Bird and 'RTV'-560 and Boneless Beef Impacts**

frequency pressure variations. Most of the high frequency signal is above 10 kHz in frequency.

The response and mode of failure of a particular component such as an aircraft windshield during impact depends on the shape and material of the windshield. For example, a thick windshield would not respond or deform grossly to the high frequency pressure variations of the impact load. The high frequency variation of the pressure would, therefore, be incapable of failing the windshield in flexure. However, delamination or spalling may occur. For a typical windshield configuration with a thickness of the order of 3 cm and a sound speed of 2 mm/μs, the double transit time across the material is approximately 30 μs. The material cannot deform appreciably for frequencies above 10-20 kHz. It was, therefore, decided to filter the pressure data above 10 kHz and record the filtered pressure (base pressure). As shown in Figure 17, filtering removes most of the high frequency component and the base or low frequency pressure remains. Present considerations center on gross deformation of windshield material and further analysis is restricted to the filtered base pressure data. It must be noted that if other failure mechanisms are considered (e.g., delamination) or different components (e.g., fan blades), then the high frequency variations may be important loading mechanisms and any analysis must recognize this.

The following parameters are identified and extracted from the filtered or base pressure-time data:

(1). Steady state pressure - the 'steady' pressure to which the pressure falls after the initial high peak.

(2). Pressure duration - measured by extending the maximum slopes of the rise and fall of pressure to the zero pressure baseline.

(3). Impulse intensity - the area under the pressure-time curve obtained by numerically integrating digitized data.

The 'steady state' pressure is indicative of the magnitude of the load imposed on the target during impact and, as the pressure-time curves have a similar shape from shot to shot, provides a convenient parameter for characterizing the pressure data. The 'steady state' pressure generated at the center-of-impact was measured for a number of shots and is plotted in Figure 18 as a function of impact velocity. The following observations are made:

(1). The 'steady state' pressure appears to be independent of bird size over the range of birds tested (0.05 kg to 0.10 kg). This supports the fluid impact model of a bird in which the pressure depends only on density and velocity and not on the size of the bird.

(2). The 'steady state' pressure is, within experimental uncertainty (largely in bird density), equal to $1/2\ \rho v^2$, as expected in incompressible fluid flow.

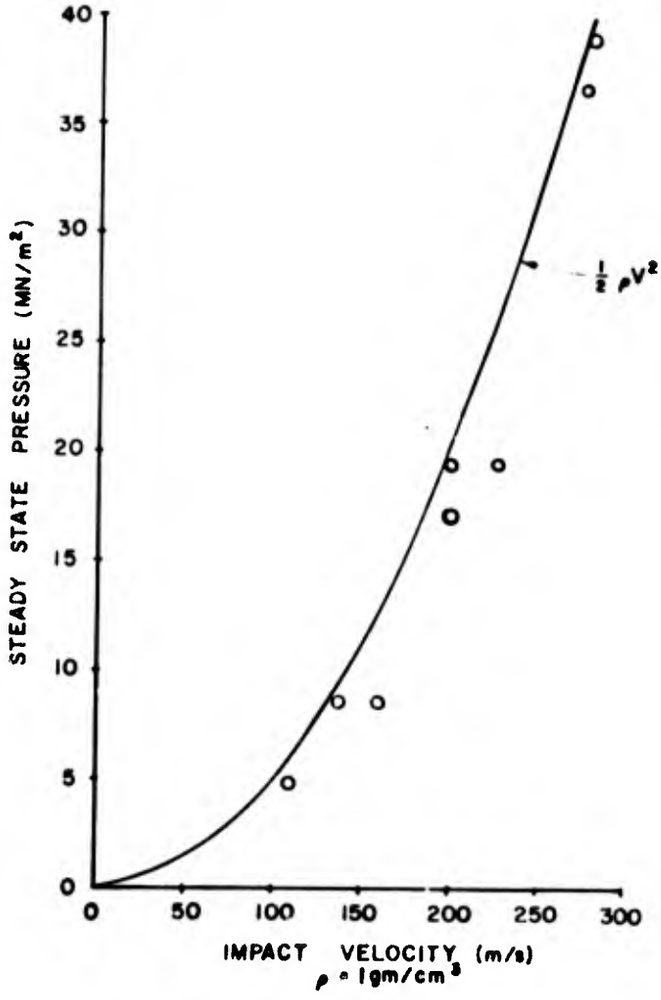


Figure 18. Steady State Pressure Vs Impact Velocity for Birds Impacted on a Rigid Plate at 90°

(3). There is considerable scatter in the data and this is attributed to nonrepeatability of bird structure, orientation at impact and center-of-impact all of which are beyond experimental control.

Pressure is measured and recorded off axis at three radii, 1.27 cm, 2.54 cm, and 3.81 cm; examples are displayed in Figure 19. This data is filtered and reduced in a similar manner to the centerline data as reported above. 'Steady state' pressures are shown plotted as a function of velocity in Figures 20 and 21. At 3.81 cm the 'steady state' pressure is essentially zero. From the data the following observations are made:

(1). The form of the pressure-time response is the same as the center-of-impact data; that is, it consists of a base pressure on which is superimposed a high frequency component. The high frequency components are filtered out for purposes as explained previously.

(2). 'Steady state' pressures are dependent on the impact velocity squared in a similar manner to the center-of-impact data and consistent with a fluid bird model.

(3). Pressure falls with increasing radial distance from the center-of-impact, as shown in Figure 22.

(4). Scatter in the data is comparable to that of the center-of-impact data and is similarly attributed to uncontrolled variations in bird structure, orientation, and location of impact.

Shot no. 5399; velocity 199 m/s; center transducer;
horizontal scale 100 μs/cm; vertical scale 24.5 $MN/m^2/cm$;
upper trace unfiltered; lower trace filtered

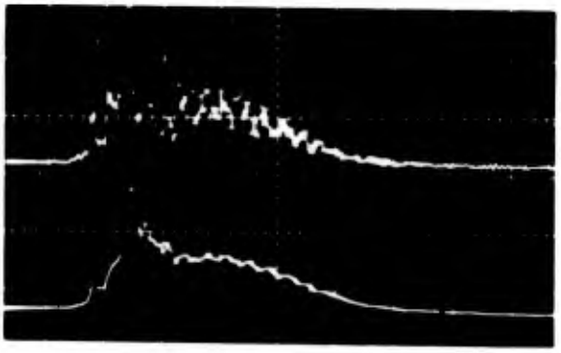

Shot no. 5399; velocity 199 m/s; transducer 12.7 mm off center;
horizontal scale 100 μs/cm; vertical scale 24.0 $MN/m^2/cm$;
upper trace unfiltered; lower trace filtered

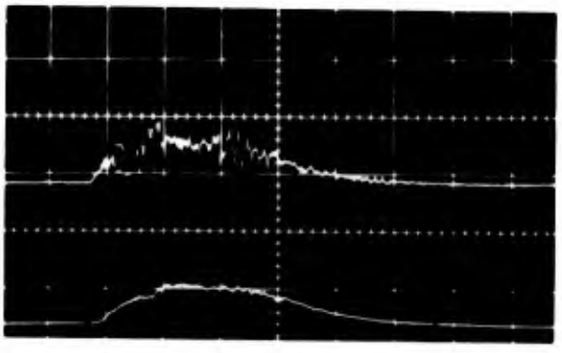

Shot no. 5399; velocity 199 m/s; transducer 25.4 mm off center;
horizontal scale 100 μs/cm; vertical scale 23.9 $MN/m^2/cm$;
upper trace unfiltered; lower trace filtered

**Figure 19. Off Axis Pressure Transducer Outputs for AFML/UDRI Target Disk**

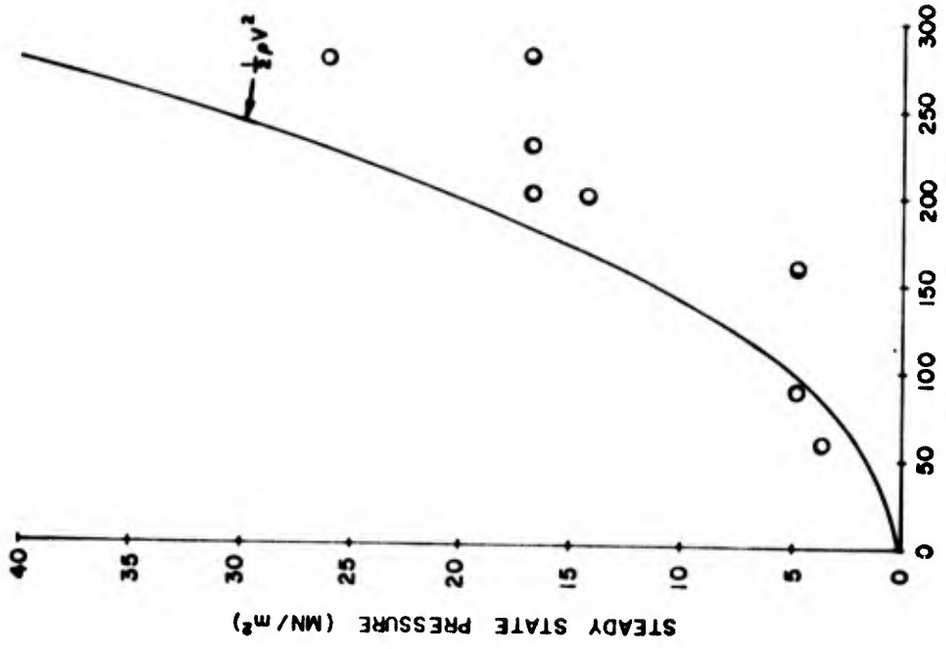


Figure 21. Steady State Pressure Vs Impact Velocity at 25.4 mm from the Center of Impact for Birds Impacting a Rigid Plate at 90°

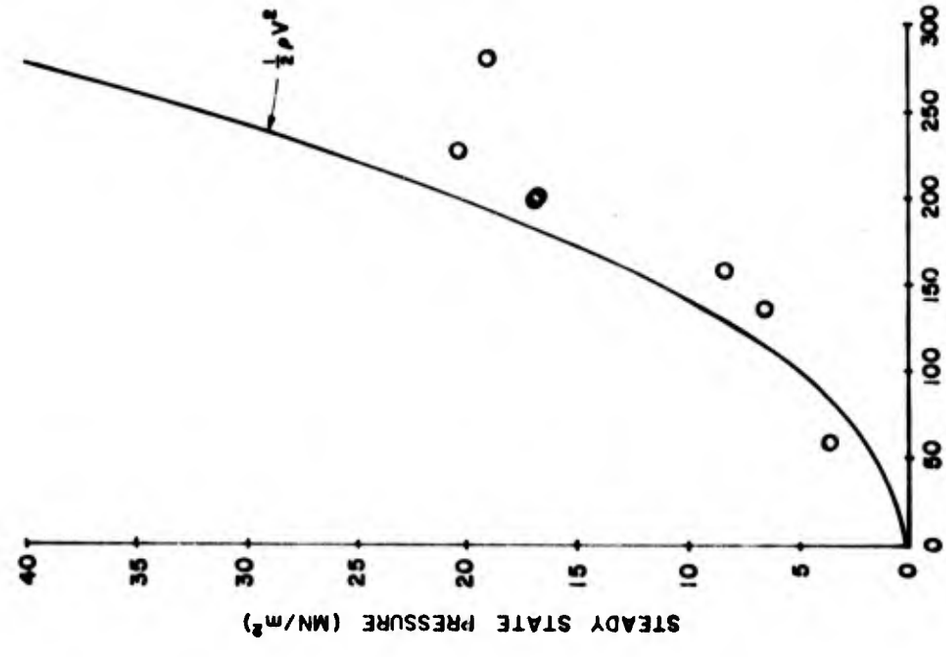


Figure 20. Steady State Pressure Vs Impact Velocity at 12.7 mm from the Center of Impact for Birds Impacting a Rigid Plate at 90°

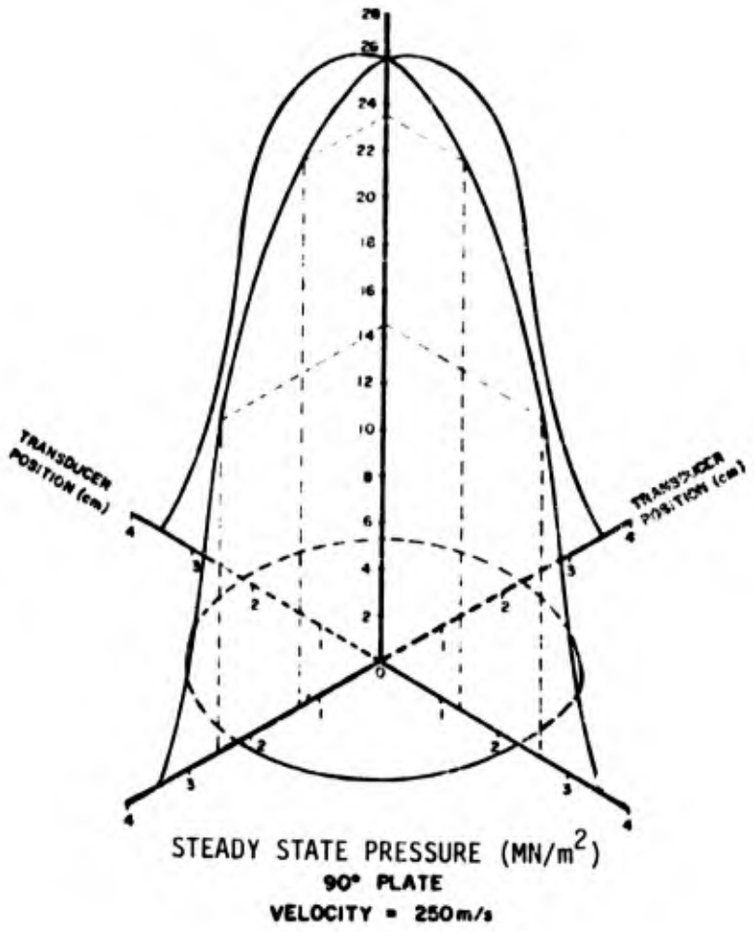


Figure 22. The Radial Distribution of Pressure for a Bird Impact on a Rigid Plate at 90°

'Steady state' pressure versus impact velocity at the center-of-impact for targets at angles of 45° and 25° are shown in Figures 23 and 24. The impact area of a bird in oblique impacts is an ellipse and pressure measurements were made at various positions along the principal axes of the impact elipse. Curves similar to those shown in Figures 23 and 24 were generated at 12.7 mm intervals along the principal axes. From these curves the spatial distribution of 'steady state' pressure is determined as shown in Figures 25 and 26.

From Figure 25 it is apparent that the maximum 'steady state' pressure occurs 'upstream' on the acute side of the impact. The pressure distribution is highly 'peaked' and the maximum 'steady state' pressure is very close to the bird 'stagnation' pressure, $(1/2\ \rho v^2)$ as shown in Figure 27.

Figure 26 indicates that at 25°, the maximum 'steady state' pressure is not nearly as high as for the 45° impacts and the distribution of pressure is more uniform (not so highly 'peaked'). The maximum 'steady state' pressure occurs above the center-of-impact on the acute side of the impact. The maximum 'steady state' pressure varies closely with the normal component of the impact velocity and is described reasonably well by $1/2\rho\ (v \sin \theta)^2$ as shown in Figure 28.

These results are consistent with the fluid model of a bird. At 90° the bird material flows out in all directions as shown in Figure 29 and at the 'stagnation' point, the steady pressure equal to $1/2\ \rho v^2$ appears. As the angle of impact obliquity decreases the bird material

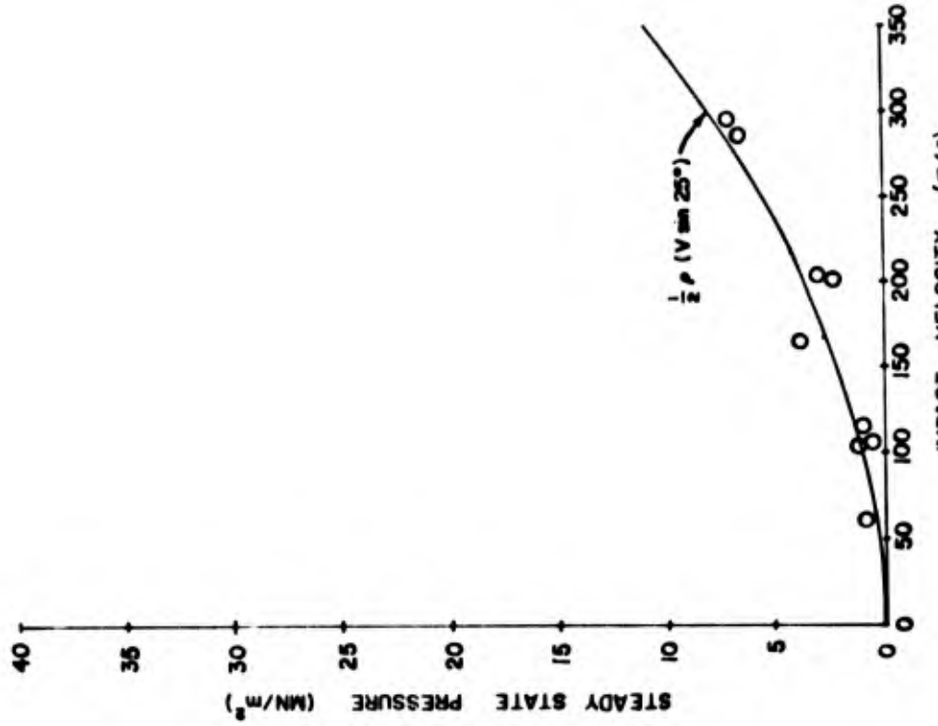


Figure 24. Steady State Pressure Vs Impact Velocity for 25° Center Impact Location

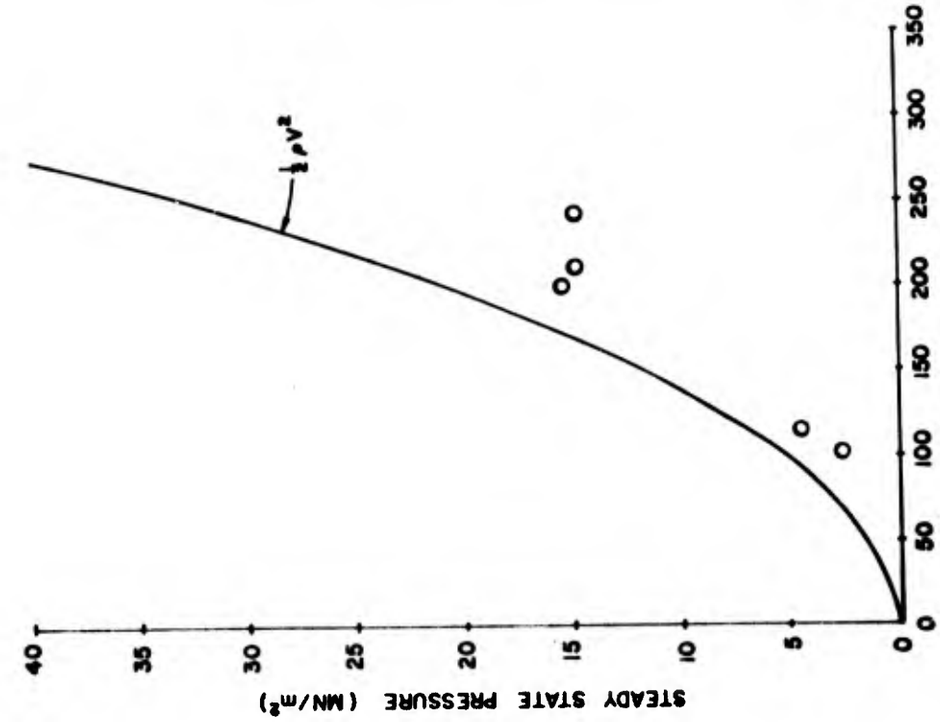


Figure 23. Steady State Pressure Vs Impact Velocity for 45° Center Impact Location

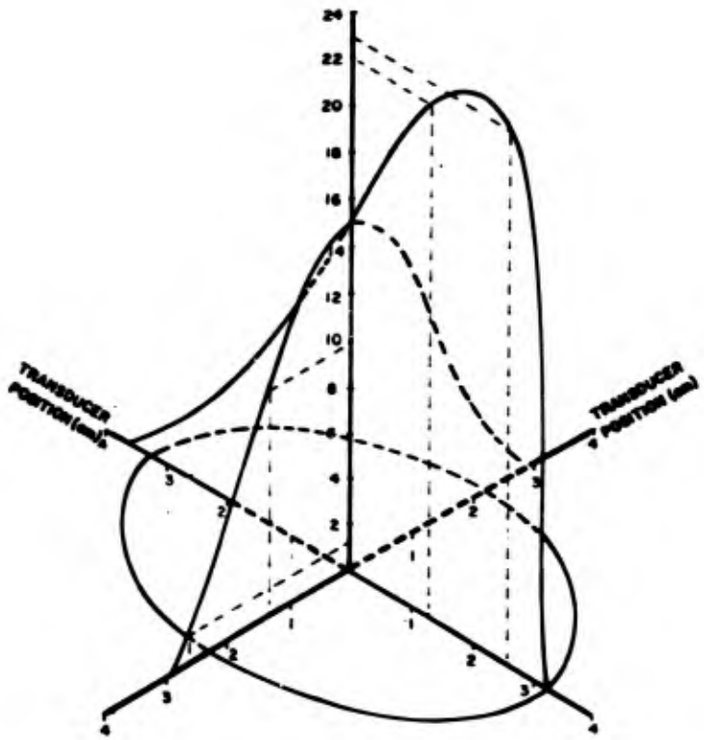


STEADY STATE PRESSURE ($MN/m^2$)
45° PLATE
VELOCITY = 250 m/s

Figure 25. Steady State Pressure Distribution Plot for a 45° Target

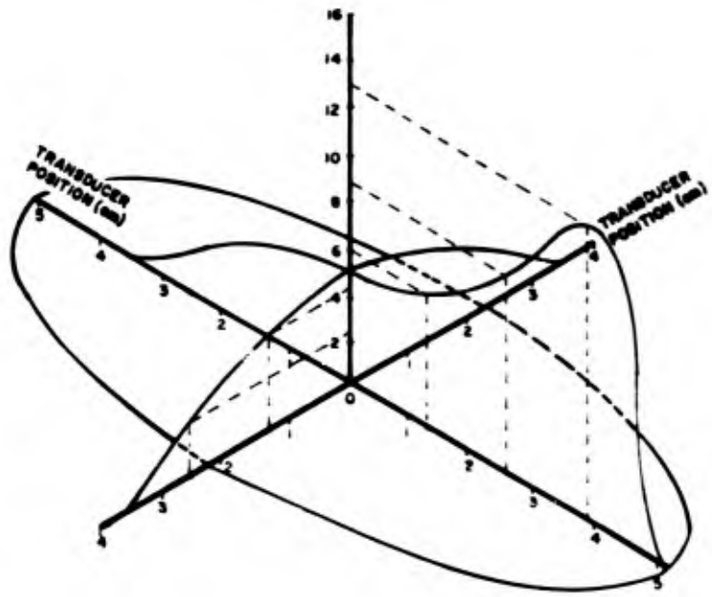


STEADY STATE PRESSURE ($MN/m^2$)
25° PLATE
VELOCITY = 250 m/s

Figure 26. Steady State Pressure Distribution Plot for a 25° Target

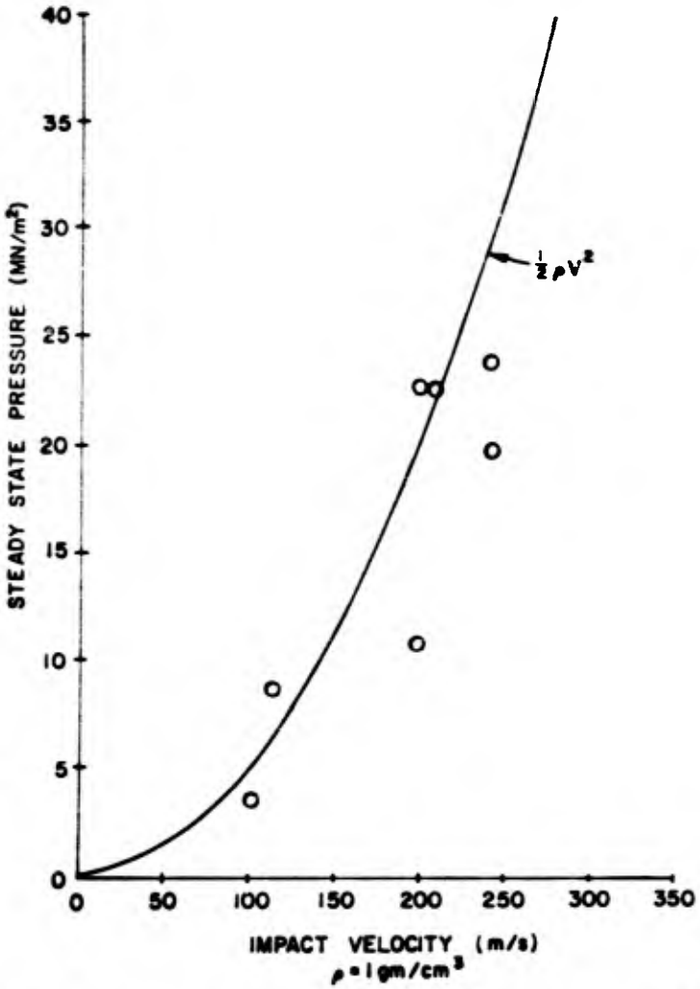


Figure 27. Steady State Pressure Vs Impact Velocity at 12.7 mm Above the Center-of-Impact for Birds Impacting a Rigid Plate at 45°

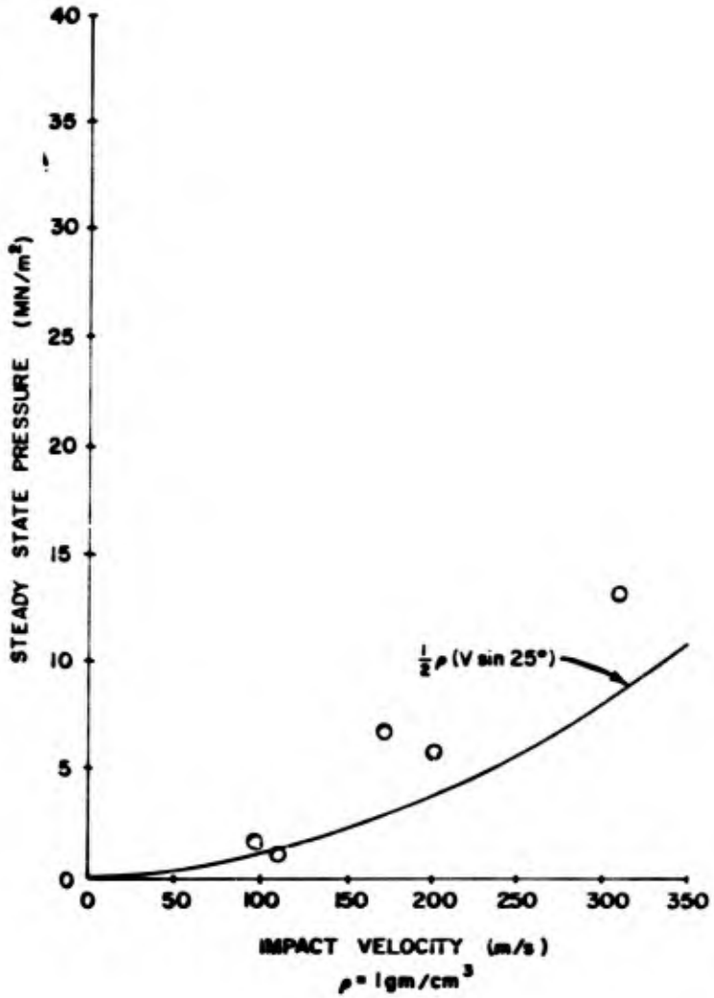


Figure 28. Steady State Pressure Vs Impact Velocity at 12.7 mm Above the Center-of-Impact for Birds Impacting a Rigid Plate at 25°

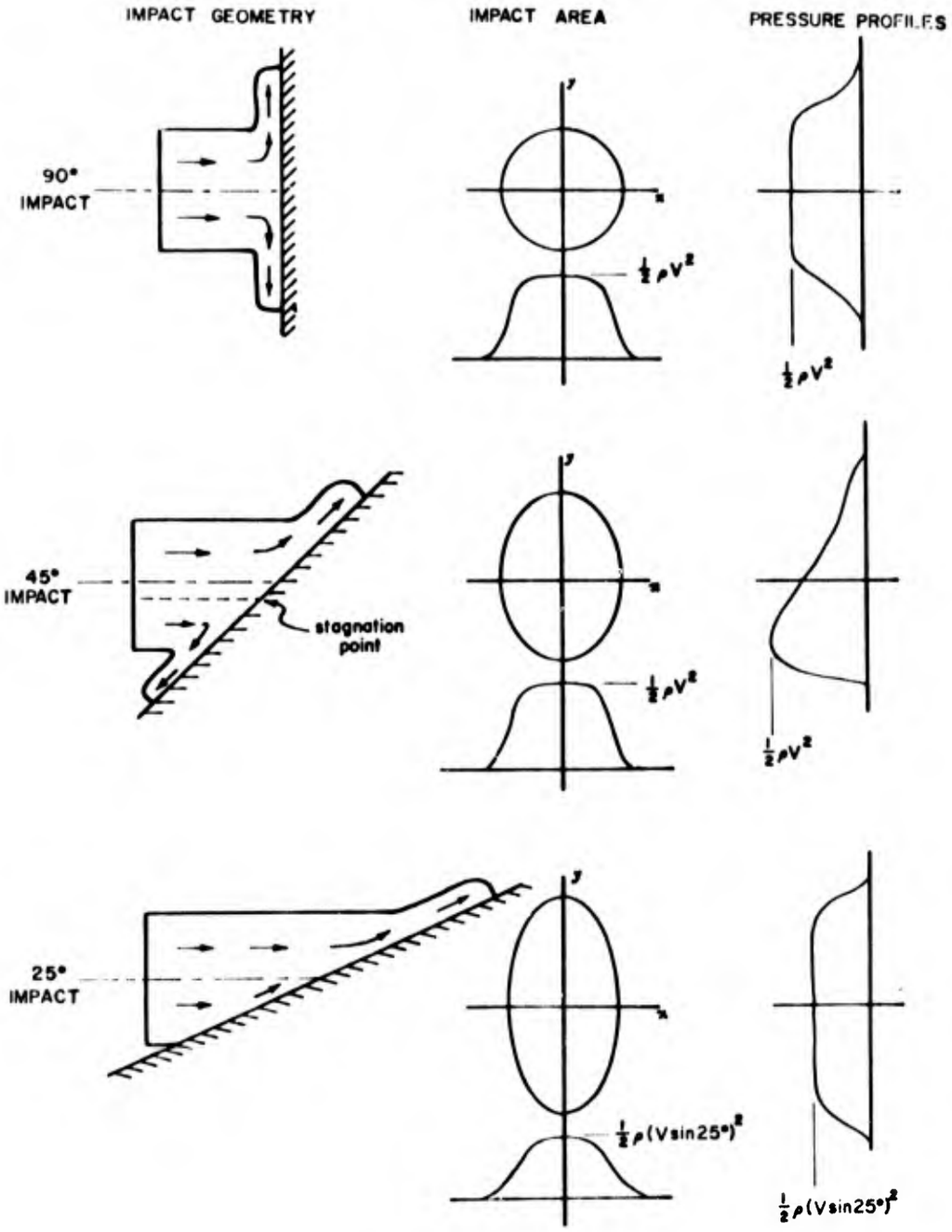


Figure 29. Bird Material Impact Geometry, Impact Area and Pressure Profiles at 90°, 45°, and 25° Impacts

still flows out in all directions as shown for the 45° impact in Figure 29. Again a 'stagnation' point appears and a steady pressure equal to $1/2\ \rho v^2$ is measured. When the obliquity falls below a certain 'critical' angle the bird material no longer flows 'upstream' as shown for the 25° impact in Figure 29. A 'stagnation' point no longer appears and the maximum 'steady state' pressure is related to the normal component of the impact velocity by $1/2\ \rho(v \sin 25°)^2$. The critical angle depends on the properties of the bird material. No 'upstream' jetting occurs when the deflected bird material travels supersonically and a shock wave forms in the bird material at the impact point. For birds the critical impact angle is apparently between 45° and 25°.

Impulse intensity for 90° impacts has been investigated. Impulse intensity is defined as the integral of pressure with respect to time and indicates the transfer of momentum to a local area in the target plate. Figures 30, 31 and 32 show impulse intensity as a function of impact velocity. The radial distribution of the impulse intensity is shown in Figure 33. From these curves it is apparent that impulse intensity increases with velocity and falls roughly sinusoidally from the center-of-impact to the nominal edge of impact.

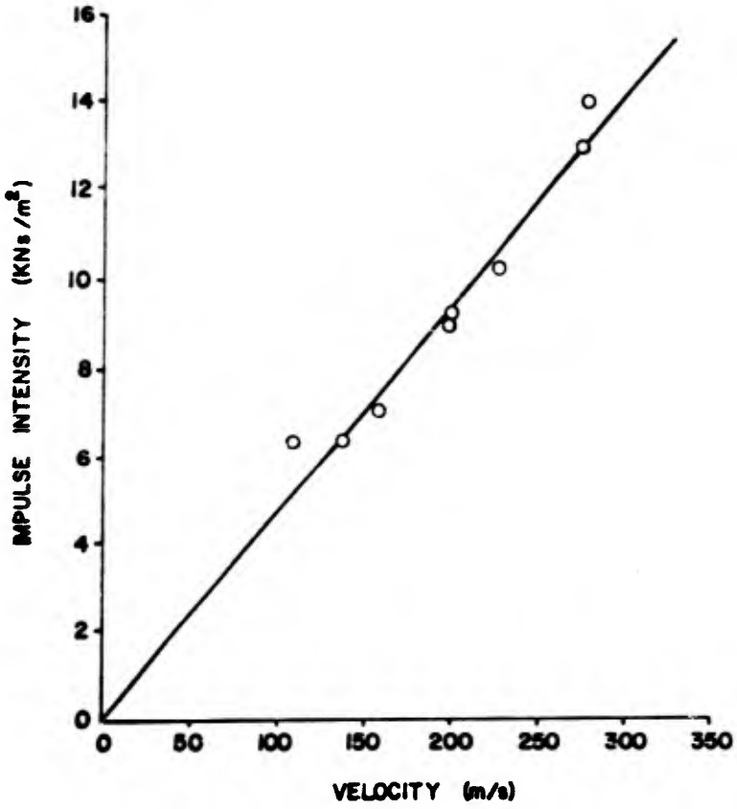


Figure 30. Impulse Intensity ($\int P\,dt$) Vs Impact Velocity at Center-of-Impact for 90° Impact

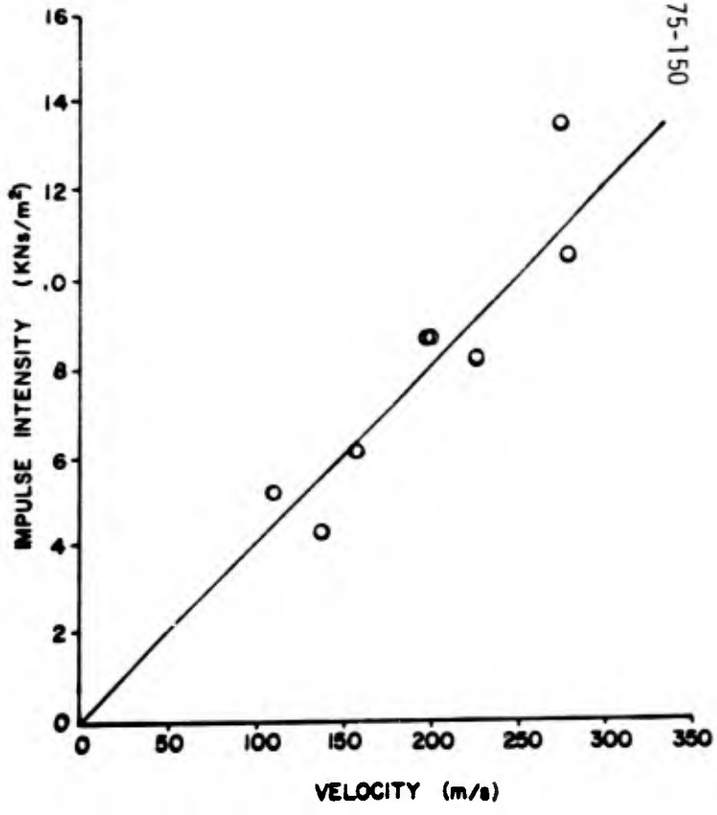


Figure 31. Impulse Intensity ($\int P\,dt$) Vs Impact Velocity at 12.7 mm from Center-of-Impact for 90° Target

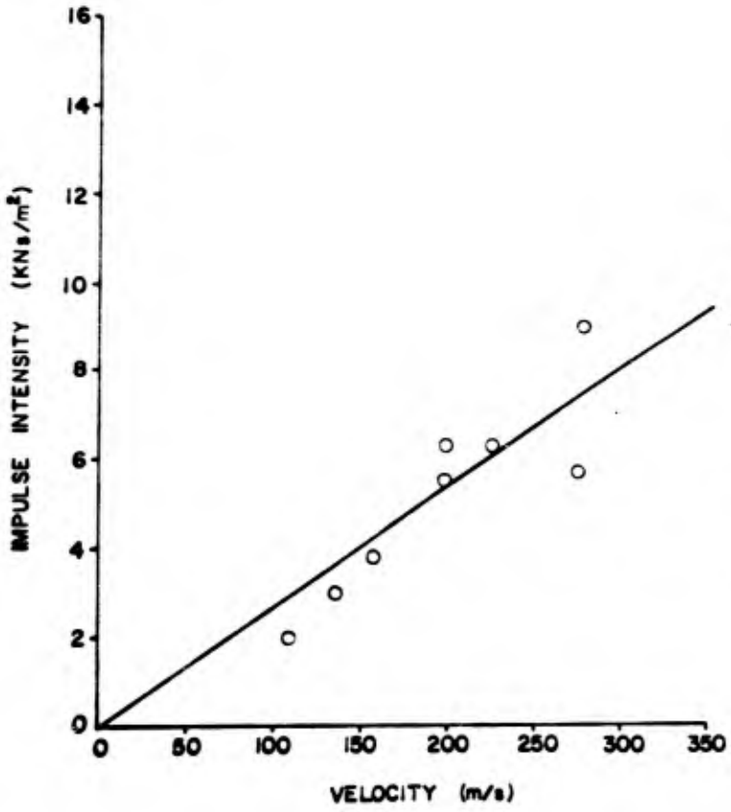


Figure 32. Impulse Intensity ($\int P\,dt$) Vs Impact Velocity at 25.4 mm from Center-of-Impact for 90° Target

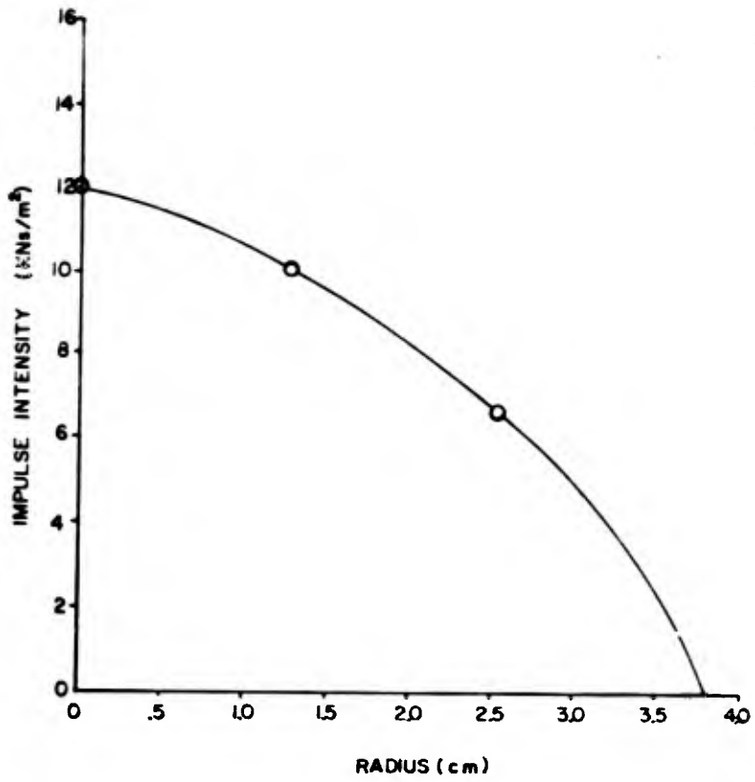


Figure 33. The Radial Distribution of Impulse Intensity for Birds Impacting a Rigid Target at 90° at 250 m/s

## 2. AEDC RESULTS

A total of 66 impact tests (21 data shots) at the 90° target angle have been conducted. The nominal test velocities are 91 m/s and 152 m/s and the nominal projectile weights are 0.9 kg, 1.8 kg, 2.7 kg and 3.6 kg. The output from the pressure transducers with appropriate in-line amplifiers and couplers are recorded on FM magnetic tape. Pressure versus time records for test number BP-43 at pressure transducer locations P-1, 2, 5, 9, 12, 13, 15, 18, 19, 21, 22, 24, 25, 27, and 30 (reference Figure 10) are shown in Figures 34 through 37. The test velocity and projectile weight for BP-43 were 91 m/s and 1.9 kg, respectively. Maximum peak pressure of 113 $MN/m^2$ occurs at location P-30, and the average pressure equals 5.5 $MN/m^2$.

On the AEDC data a 'steady state' pressure is difficult to identify as the pulse durations are relatively long and the pressure appears to fall steadily during the impact. At this time, insufficient data has been analyzed to determine if this is a real size scaling effect. Instead of 'steady state' pressures, average pressures, defined as the impulse intensity divided by the duration, are determined.

The total impulse imparted to the target is calculated by multiplying the impulse intensity by the effective area monitored by eacn transducer and adding the results for all the transducers together.

a. Comparison of AFML/UDRI and AEDC Results - The average pressure as determined from the AEDC tests is plotted together with the 'steady state' pressure from AFML/UDRI results for the center-of-impact at 90° in Figure 38. If the initial pressure spike does not contain a significant portion of the impulse intensity (this appears to be true in the AEDC data) the two sets of data should agree as demonstrated in Figure 38. The data now covers a range of bird masses from 0.05 kg to 3.60 kg, over a factor of 70, and the magnitude of the pressures generated at impact are, as expected, independent of bird size.

The impulse imparted to the target as a function of impact momentum is shown in Figure 39. As expected, the impulse is equal to the impact momentum within the measurement uncertainty. Again, the AFML/UDRI and AEDC data agree and indicate negligible bird bounce.

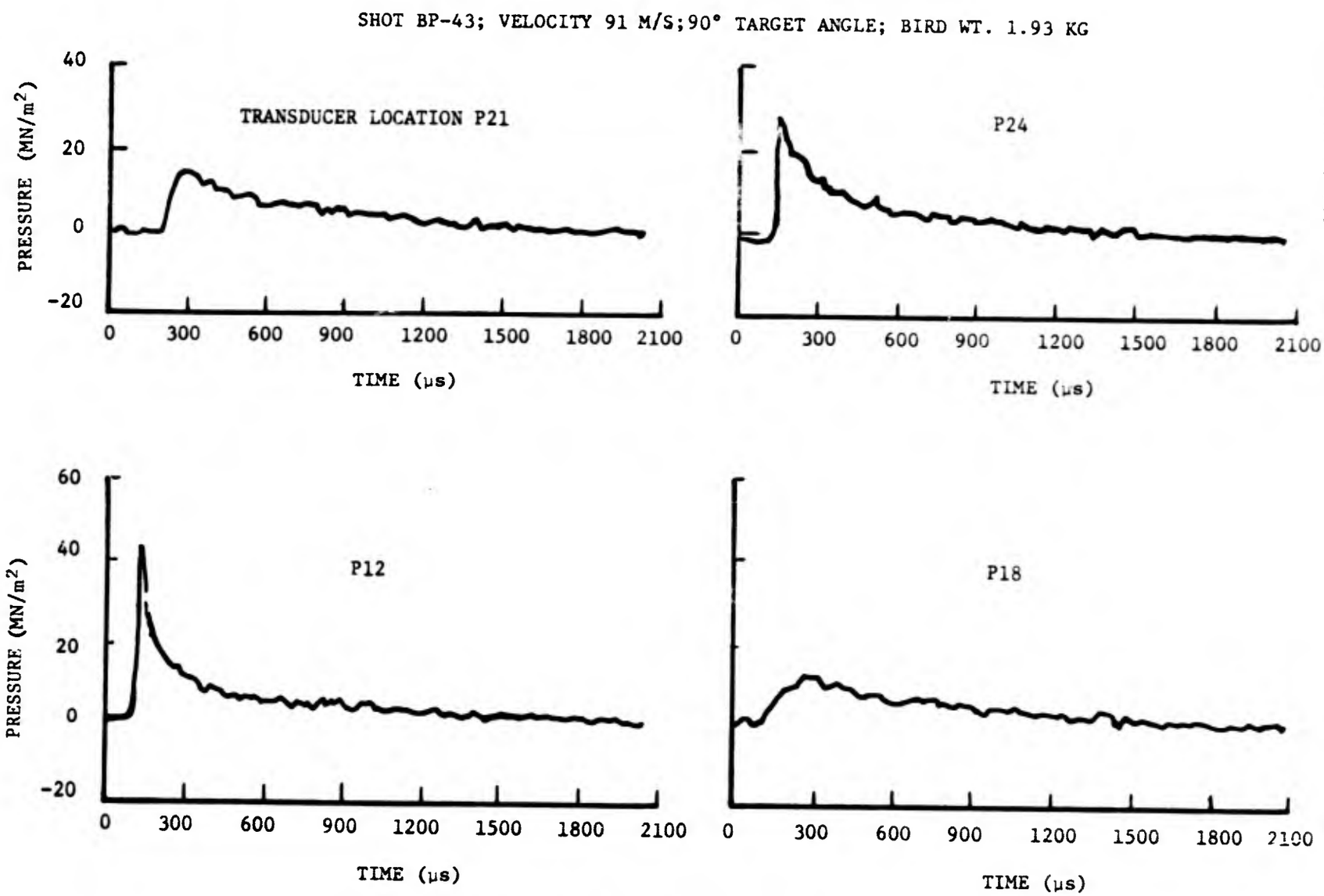


Figure 34. Pressure as a Function of Time for Transducer Locations P12, P18, P21, and P24

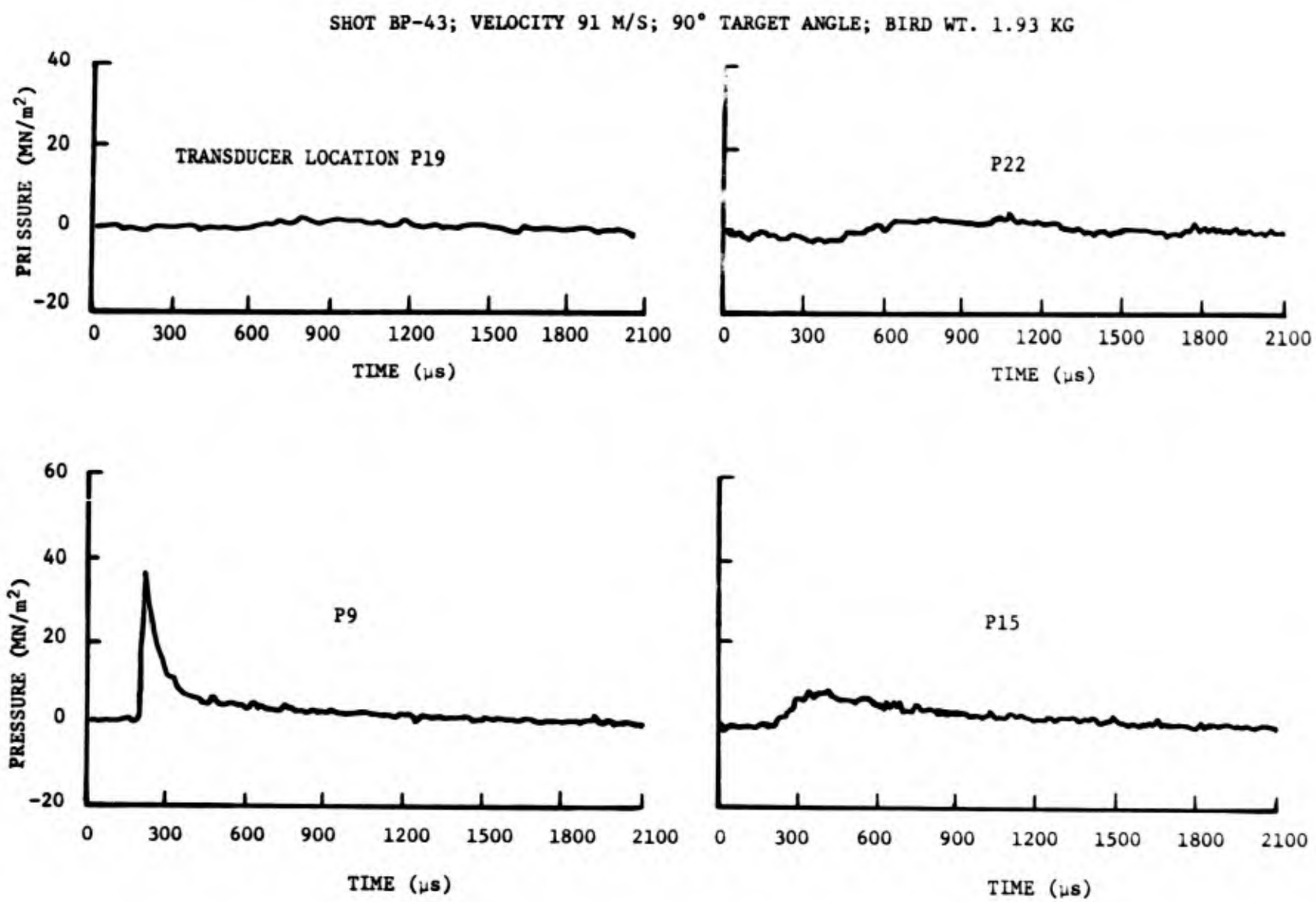


Figure 35. Pressure as a Function of Time for Transducer Locations P9, P15, P19, and P22

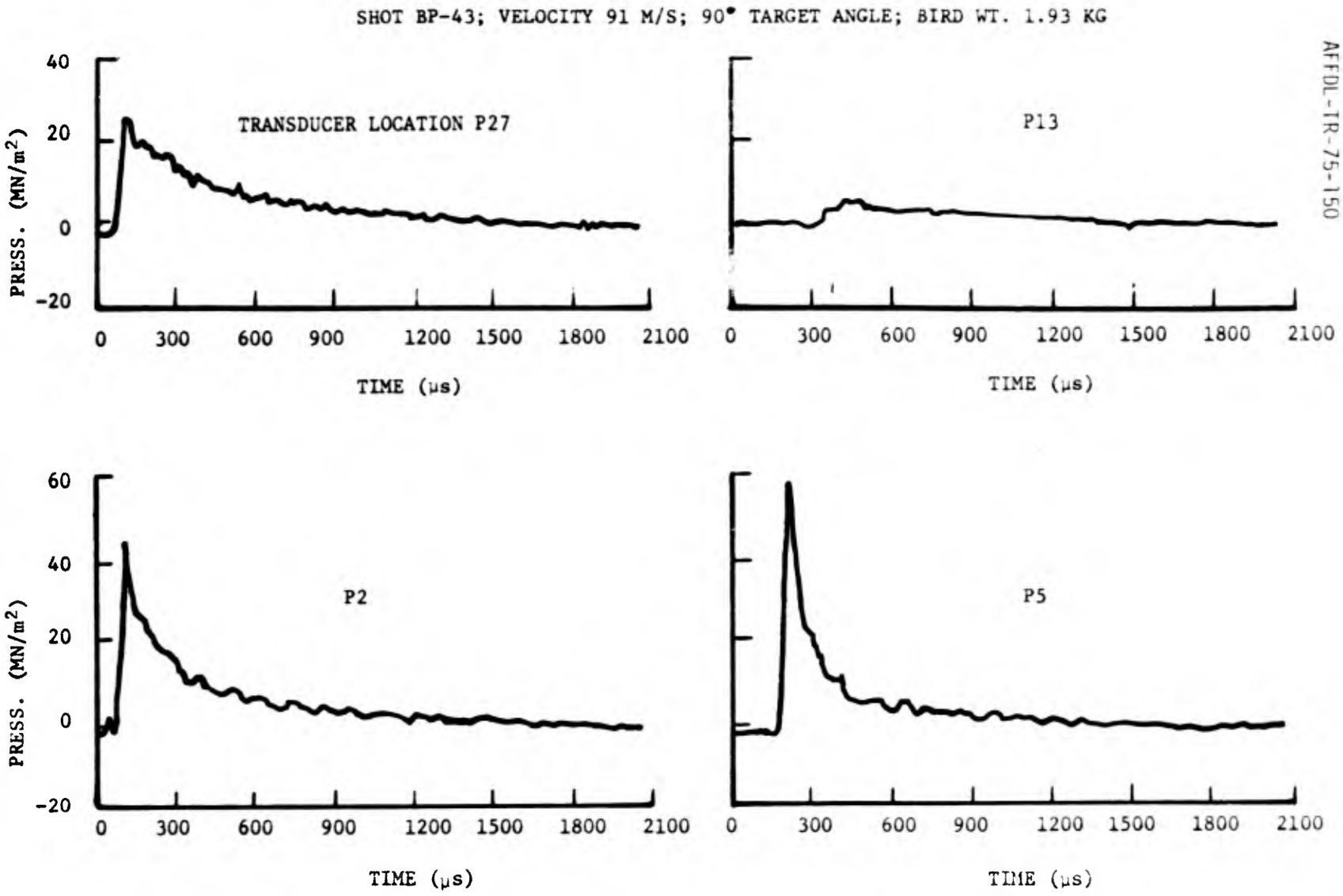


Figure 36. Pressure as a Function of Time for Transducer Locations P2, P5, P13, and P27

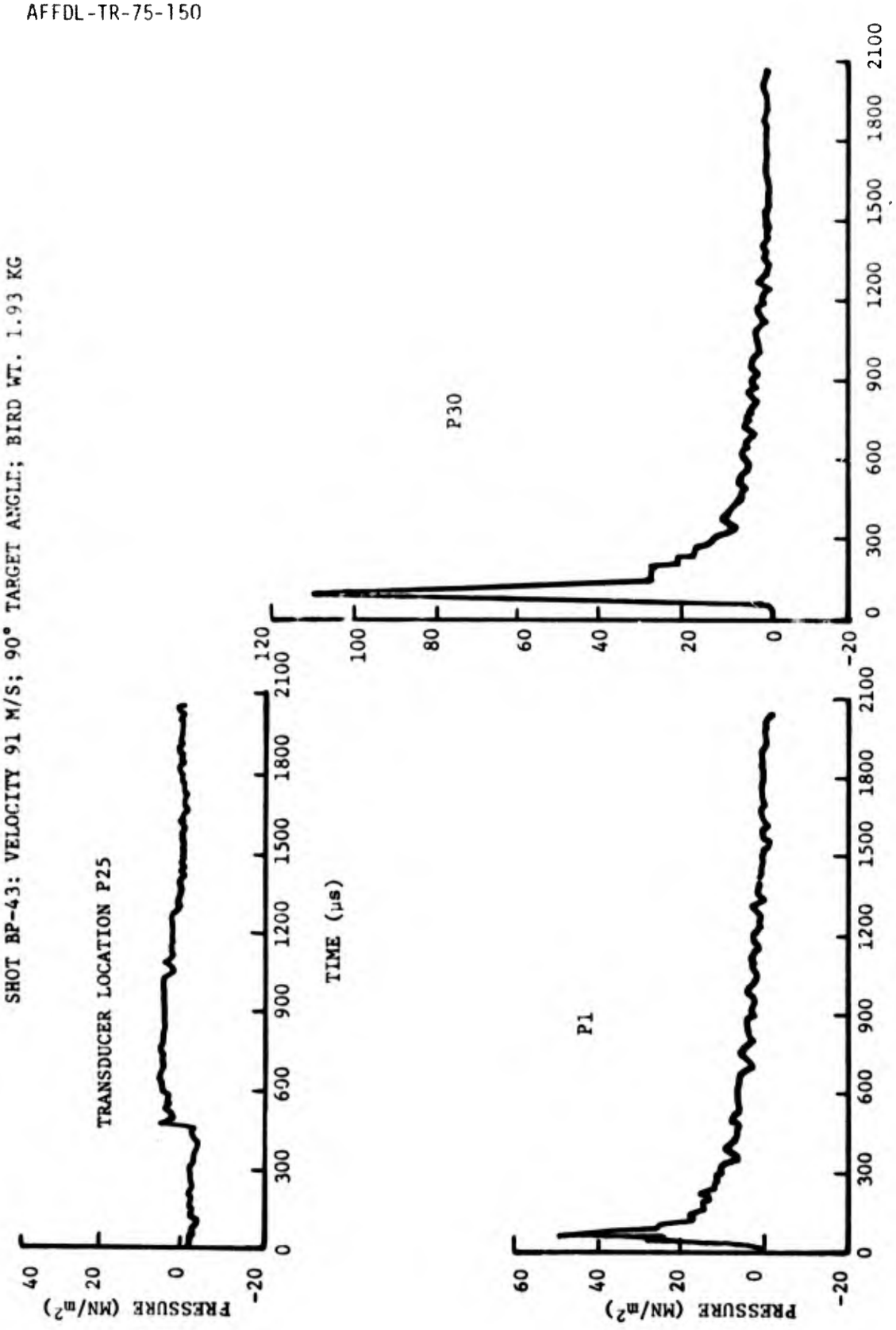


Figure 37. Pressure as a Function of Time for Transducer Locations P1, P25, and P30

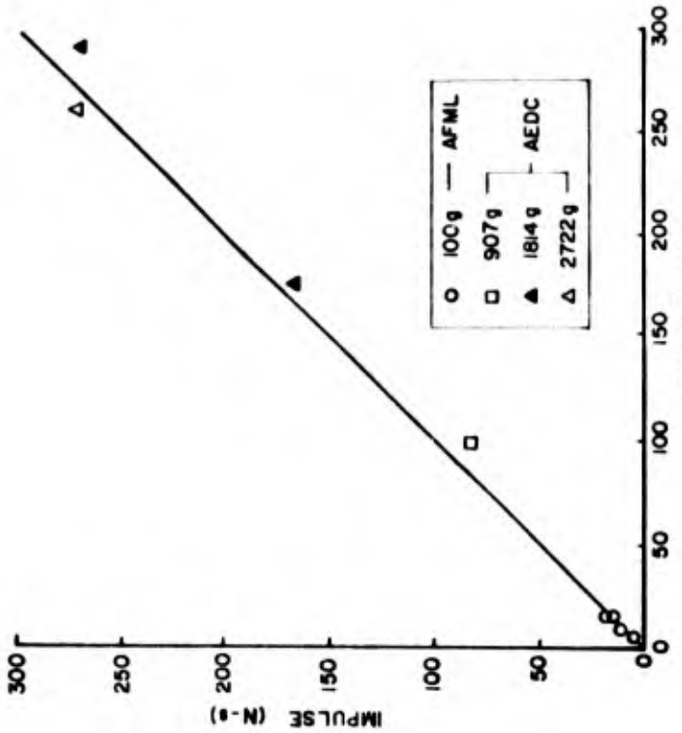


Figure 39. Comparison of AFML/UDRI and AEDC Impulse Vs Momentum

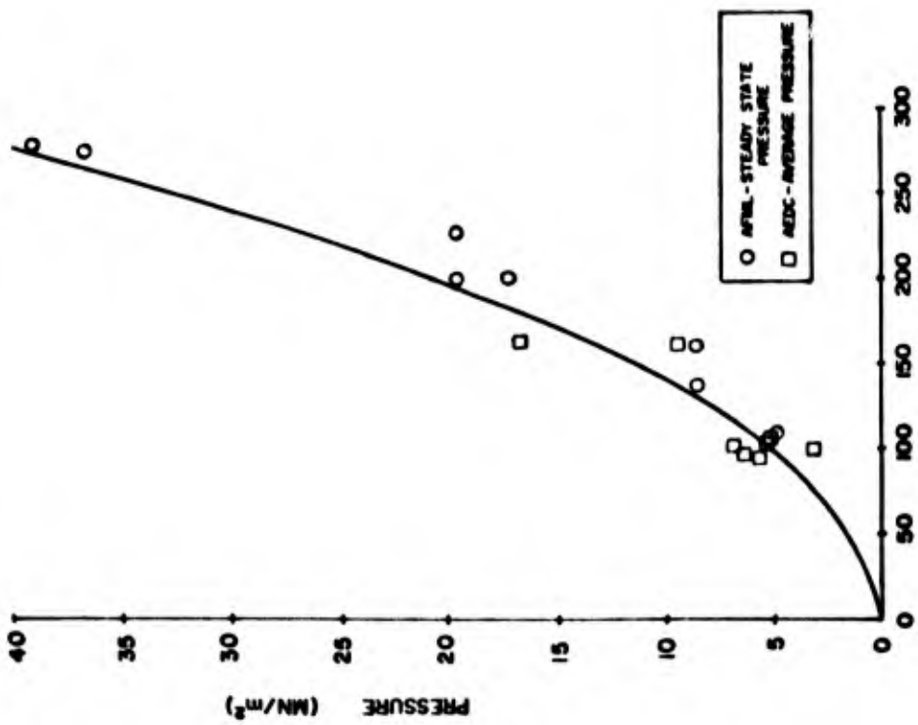


Figure 38. Comparison of AFML/UDRI and AEDC Pressure Vs Impact Velocity for the 90° Center-of-Impact

# SECTION IV

# CONCLUSIONS

From the experimental data collected and analyzed to date a number of important conclusions may be drawn.

## 1. Hopkinson Bar Results

From the Hopkinson bar measurements it is seen, for a rigid plate impact, birds display negligible bounce. That is, the impulse imparted to the target is equal to the impact momentum.

The duration of the total force-time pulse is closely approximated by the 'squash up' time (the length of the bird divided by the impact velocity). Therefore the average force exerted during the impact is given by the momentum divided by the 'squash up' time. The measured peak force is shown to be very nearly twice the average, and the force-time pulse is approximately 'triangular.'

Integration of the AEDC measurements to derive total force versus time yields similar results, but insufficient data has been collected and reduced to completely verify this behavior for very large birds.

## 2. Pressure Plate Results

The pressure plate measurements indicate clearly that the birds behave as a fluid during impact. The impact process may be described as the nonsteady flow of a finite cylinder of matter on the plate surface.

At the instant of impact, a plane shock wave propagates into the bird. This plane shock wave generates very high initial pressures approximately equal to the uniaxial strain or Hugoniot pressure. Rarefaction waves rapidly travel in from the edges of the bird and attenuate the pressures at the center of impact. The pressure decays to the steady flow 'stagnation' value given by the density times the velocity squared divided by two, where the apparent density of the bird is somewhat less than 1 $g/cm^3$.

As the obliquity of impact is decreased a critical angle is reached at which bird material no longer flows out in every direction. The maximum 'steady state' pressure then falls to reflect only the normal component of impact velocity. For example at 45°, which is apparently above the critical angle, the maximum 'steady state' pressure is the full 'stagnation' pressure (the same as for a 90° impact). At 25°, which is below the critical angle, the maximum 'steady state' pressure falls to $(\text{Sin } 25°)^2$ of the 'stagnation' pressure.

The 'steady state' pressure is independent of bird size.

The pressure is exerted over approximately the nominal impact area of the bird. The pressure is highest at the center-of-impact (or slightly 'upstream' for oblique impacts) and falls off gradually towards the edges of the bird.

There is considerable high frequency component in the bird pressure pulse. This high frequency variation is attributed largely to the breakup of the flesh with contributions from inhomogeneities in the bird.

3. Future Work

The analysis of oblique impact pressure data is not yet complete and this work is continuing. No large bird data from AEDC is available as yet on oblique impacts and this data will be obtained.

Oblique impact Hopkinson bar tests will be conducted at AFML/UDRI to address the question of total force variations with impact obliquity.

The measurements reported herein and the additional work noted above are limited by the rigid plate technique. Real aircraft components subjected to birdstrike are not rigid, the effects of target compliance must be addressed. An investigation of the coupling between bird impact loading and target response will be undertaken in the near future.

## REFERENCES

1. Barber, John P., Taylor, Henry R., and Wilbeck, James S., Characterization of Bird Impacts On A Rigid Plate: Part I, Air Force Flight Dynamics Laboratory Report No. AFFDL-TR-75-5, January 1975.

2. Sanders, E. J., The AEDC Bird Impact Test Facility, Air Force Materials Laboratory Report No. AFML-TR-73-126, PP 493 through 514, June 1973.



☆ U. S. GOVERNMENT PRINTING OFFICE: 1976 — 657-650/602